THESIS APPROVAL

GRADUATE SCHOOL, KASETSART UNIVERSITY

Master of Engineering (Electrical Engineering)

DEGREE

Electrical Engineering	Electrical Engineering
FIELD	**DEPARTMENT**

TITLE: Vibration Suppression of Flexible Robot based on Resonance Ratio Control with Coefficient Diagram Method

NAME: Mister Phalakorn Kladjaroen

THIS THESIS HAS BEEN ACCEPTED BY

THESIS ADVISOR

(Mr. Chowarit Mitsantisuk, D.Eng.)

DEPARTMENT HEAD

(Assistant Professor Wachira Chongburee, Ph.D.)

APPROVED BY THE GRADUATE SCHOOL ON

DEAN

(Associate Professor Gunjana Theeragool, D.Agr.)

THESIS

VIBRATION SUPPRESSION OF FLEXIBLE ROTBOT BASED ON RESONANCE RATIO CONTROL WITH COEFFICIENT DIAGRAM METHOD

PHALAKORN KLADJAROEN

A Thesis Submitted in Partial Fulfillment of
the Requirements for the Degree of
Master of Engineering (Electrical Engineering)
Graduate School, Kasetsart University
2014

Phalakorn Kladjaroen 2014: Vibration Suppression of Flexible Robot based on Resonance Ratio Control with Coefficient Diagram Method. Master of Engineering (Electrical Engineering), Major Field: Electrical Engineering. Thesis Advisor: Mr. Chowarit Mitsantisuk, D.Eng. 61 pages.

Generally, the industrial machine and robot manipulator with the flexible tool is used in many applications, such as the high-resolution milling and the complex surgery. The force sensors are used to measure the external force, which is the force feedback in the force control. However, the force sensor has too many disadvantages, for example, the noise and the limit bandwidth. To solve these problems, a disturbance observer (DOB) is used to estimate the external force, but it is not work in more than one-mass system. Because the external force entered multi-mass system on the load side. So a multi-encoder based on disturbance observer (MEDOB) is used to estimate the external force in the flexible robot.

In multi-mass system, it consists many mass connected by the flexible structure that made the vibration in the system. A resonance ratio control is applied to suppress the vibration in the system, because the conventional controller cannot control this system. Then, the optimum control parameters of the resonance ratio control is designed by a coefficient diagram method (CDM) for the robustness of the system. In addition, the bilateral control will have the best performance if the vibration does not occur in the system and the estimate of force is precise and accurate.

The effectiveness of this method is verified by numerical simulation results. By using the proposed method, the vibration effect can be rejected very successfully in the flexible robot system. In addition, the force and position responses of this method is better than the conventional methods.

_____ _____ ___ / ___ / ___

Student's signature Thesis Advisor's signature

ACKNOWLEDGMENTS

I would like to express my sincere thanks to my thesis advisor, Dr. Chowarit Mitsantisuk for his invaluable help and constant encouragement throughout this research. I am most grateful for his teaching and advice, not only the research methodologies but also many other methodologies in life. I would not have achieved this far and this thesis would not have been completed without all the support that I have always received from him.

In addition, I am grateful for the teachers of electrical engineering: Dr. Komsan Hongesombut and others person for suggestions and all their help.

Finally, I most gratefully acknowledge my parents and my friends for all their support throughout the period of this research.

Phalakorn Kladjaroen

July 2014

TABLE OF CONTENTS

Page

LIST OF TABLES

LIST OF FIGURES

LIST OF FIGURES (Continued)

LIST OF ABBREVIATIONS

DOB	=	a disturbance observer
MEDOB	=	a multi-encoder based on disturbance observer
CDM	=	a coefficient diagram method

VIBRATION SUPPRESSION OF FLEXIBLE ROBOT BASED ON RESONANCE RATIO CONTROL WITH COEFFICIENT DIAGRAM METHOD

INTRODUCTION

Recently, the robots are widely used in applications such as industrial machine tool, advanced medical devices and precision assembly equipment, as well as in the car manufacturing assembly process, since they are enable economical, high accuracy, and high precision. By using the gear-box or harmonic drive, the effectiveness in the applications is low, because the robots have the flexible structure. Generally, the force sensors are applied to measure the external force and feed it back to the control system. However, force sensors have not high bandwidth and have a noise, which is a significant cause of instability in the system. The main component of force sensor is the strain gauge. Therefore, it is necessary to compensate the vibration effect due to the flexibility of strange gauge in the controller design. The quality of the force sensors is due to its cost. Moreover, the force sensors can measure only the tip position, which it is implemented. Consequently, a disturbance observer has been used, not only for improving the robustness and bandwidth of the control system, but also for estimation the external force.

In this thesis, a novel bilateral control is proposed for a high stability and vibration suppression of flexible master-slave robot in bilateral control. By using the resonance ratio control with coefficient diagram method (CDM), it is possible to transmit the force sensation from the master robot to the slave robot without the oscillation. The velocity response at the slave side can be tracked almost identically over the velocity response at the master side. From the simulation results, a high performance of the position and force control can be achieved by applying the proposed controller design. The simulation results are provided to illustrate the performance of the proposed algorithms. These proposed algorithms can be applied in the factory industry and the surgery in the difficult part to access.

OBJECTIVES

The objectives of this study are as follows:

1. To estimate force in the flexible robot without using the force sensors.

2. To apply the resonance ratio control in the flexible robots, which are two, and three-mass system.

3. To design the optimal coefficient of controller by using the Coefficient Diagram Method (CDM).

4. To reduce vibrations in the bilateral control system of the flexible master-slave robot in the two-mass system.

LITERATURE REVIEW

The research topics to control of master-slave robots for working in the bilateral control system has been challenge in many researches in this area in recent years. Robots in the master-slave configurations have been proposed to perform tasks in many application areas (see, for example, (Garcia *et al.*, 2008; Tsuji *et al.*, 2009; Yalcin and Ohnishi, 2009; Yokokura *et al.*, 2009; Abeygunawardhana and Murakami, 2010; Brigante *et al.*, 2011; Linda and Manic, 2011; Mitsantisuk *et al.*, 2012a; Strolz *et al.*, 2011)). The bilateral control supplies force feedback from the slave robot to the human operator through the master robot. On the other hand, a slave robot is applied to interact with unknown environments. Both of master and slave robots are bilaterally controlled with force and motion movements. In the bilateral control system, the master and slave robot have the same structure and sensor unit. In order to make the robot system has a high performance, flexible, and applicable, the different types of motor and sensor have to designed and constructed. For example, the robot arm on the mobile robot is controlled to operate the complex tasks by a joystick at the master side. This way, the mobile robot at the slave side is used to operate and interact with open environment. However, the problems of flexible robot system, such as undesirable oscillations and instability, reduce the performance not only at the slave side but also at the whole system. In order to develop the bilateral control system, the method, which is used to control the robot to contact with an unknown environment. Therefore, it is difficult to design the controller of this system.

Generally, a force sensor has been widely applied to measure the external force (Oishi *et al.*, 1984; Ferretti *et al.*, 2004; Jaechan and Hong, 2010; Puangmali *et al.*, 2010; Salvatore *et al.*, 2010; Suwanratchatamanee *et al.*, 2011). However, the force sensor has a low bandwidth since the strain gauge with soft structure and it has too much noise. Moreover, the deterioration of using force sensor is the presence of significant oscillation in the system (Katsura *et al.*, 2007). To fix the disadvantage of the force sensors, based on the sensorless force control technology, a state observer is used to estimate unknown state variables (Ohba *et al.*, 2009). Many practical application systems have confirmed that the state observer can be used to instead of

the real force sensor(Back and Shim, 2008). However, the exact parameters of the observer are difficult to obtain. A disturbance observer (DOB) is become a preferred approach for improving robustness and accuracy of the force estimation of the control system.(Yuki *et al.*, 1993; Katsura *et al.*, 2008; Kubo and Ohnishi, 2009; Natori *et al.*, 2010; Mitsantisuk *et al.*, 2012b). It shows that superior performance with robustness can be achieved by using the DOB. The DOB is simple to design and easy to implement since a complicated identification of the parameter, which is not required. The motor's current and velocity are the reference input of the DOB, whereas the external force estimation is the output.

Although the DOB and the state observer offer a simple way to estimate the external force, it is not suitable to apply in the robot, which consists of a motor M and a load L, connected by a flexible structure to transmit the actuator torque to a distant joint. Since the actuator is connected to the load side with a transmission mechanism, its elasticity causes resonance in the system. Therefore, the elasticity of flexible robot is realized under assumptions, which is model, by spring coefficient Ks and mass system. Because of the advantages and unique features of disturbance observer, this approach has received much attention in sensorless force control system. Instability and vibration of system can occur when using disturbance observer for the two-mass system because of the presence of spring that reduce the overall performance. In order to solve these problems, a load disturbance observer (LDOB) is proposed to estimate the external force on the load side. However, the exact parameters of the spring coefficient is difficult to obtain (Katsura *et al.*, 2006). Moreover, it can be assumed by using a non-linear relationship. In order to address these problems, a multi-encoder-based disturbance observer (MEDOB) is proposed for estimating the external force at the load side of flexible robot.(Mitsantisuk *et al.*, 2012c).

Generally, the conventional PID controller is widely used in the industrial machines. Although this method offers a simple way to design the controller, it is not perform well when the plant system is unstable or has a resonance structure. Therefore, it is necessary to design the controller for guarantees the robustness and suppresses vibration. To control machine with the resonance structure received more

attention from the researcher (Pereira *et al.*, 2011; Mitsantisuk *et al.*, 2012c). A new effective control method, the resonance ratio control has been proposed to improve the robustness and suppress the oscillation during task executions for position control system (Yuki *et al.*, 1993). This method relies on the possibility to change the virtual inertia moment in the motor side by feeding back the estimated reaction torque to the motor in an acceleration dimension. It makes the resonance frequency and the resonance ratio of the system can be changed to an arbitrarily value. In the position control, it is found that the vibration is well compensated by using the resonance ratio gain as $\sqrt{5}$. In addition, the sensorless force servoing based on resonance ratio control was proposed by Katsura (Katsura *et al.*, 2006). This method has proven itself as an excellent controller for compensate the vibration by setting the resonance ratio gain as $\sqrt{6}$. By setting these designed gains, it caused the force response has no overshoot and vibration. These, the resonance ratio parameter is calculated by using the coefficient diagram method (CDM). From the calculation, a new resonance ratio gain based on the CDM has been presented as 2.0 (Mitsantisuk *et al.*, 2012c).

In this thesis, DOB and MEDOB are applied to estimate the external force on motor side and load side of the two or three-mass system. In two – mass system, the resonance ratio control with the CDM is used to control the force in the bilateral control. The vibration of the system can be suppressed by using this method. In three – mass system, the PID controller with resonance ratio control is applied to control the system. This thesis improves the resonance ratio control with the CDM to be able to control the three – mass system.

MATERIALS AND METHODS

Materials

1. Computer

2. Program MATLAB

Methods

1. Two - mass system

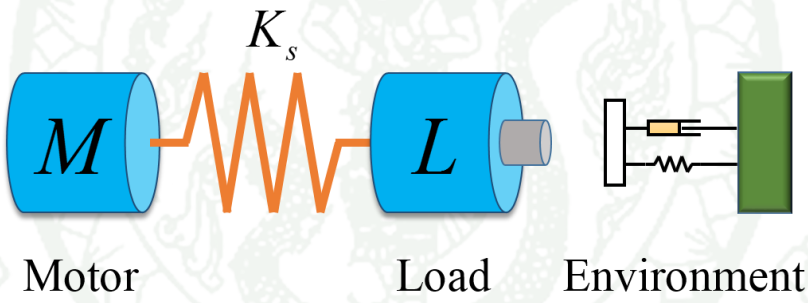

Figure 1 The model of the two-mass system.

Generally, the robot system is consist of a mass of motor M and a mass of load L, which connected together with a flexible structure to transmit the actuator torque to a distant joint. Since the actuator is connected to the load side with a transmission mechanism, its elasticity causes resonance frequency in the system. Therefore, the elasticity of flexible robot is realized under assumptions that it is modeled by constant spring coefficient K_s and mass system, which is called the two-mass system, as shown in Figure 1.

A block diagram of the two-mass system, which controls under the ideal current source, is shown in Figure 2. The dynamic equation of the linear motor can be described by:

$$\ddot{X}_m = -\frac{K_s}{M} X_s + \frac{K_t}{M} I_m \tag{1}$$

$$\ddot{X}_l = \frac{K_s}{L} X_s - \frac{1}{L} F_{dl} \tag{2}$$

$$\dot{X}_s = \dot{X}_m - \dot{X}_l \tag{3}$$

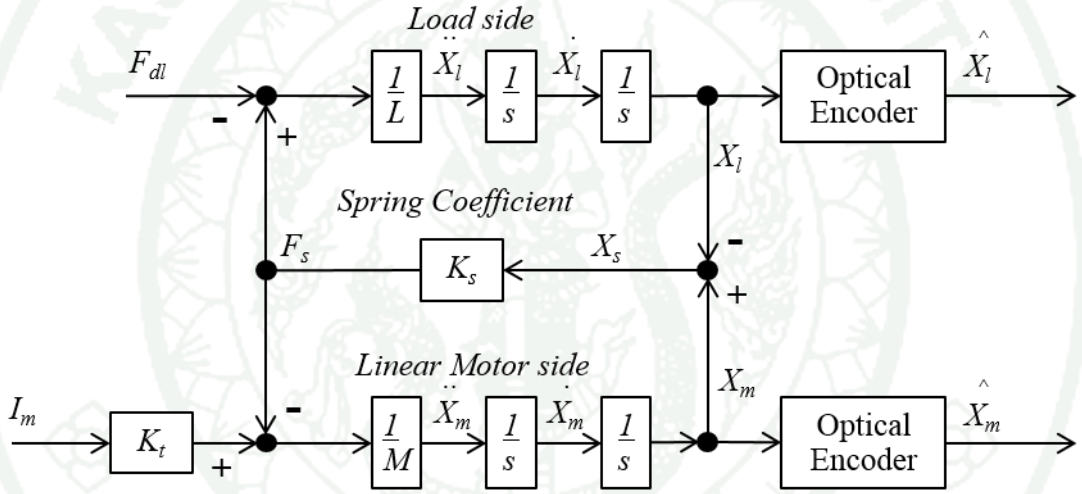

Figure 2 The block diagram of the two-mass system.

where subscripts m and l denote the motor side and load side, respectively. F_s and F_{dl} are the spring force and the external force on the load side. K_t is the force coefficient, I_m is the current, X_s is the torsional position from the position of the motor X_m and the position of the load X_l, $\ddot{X}$ is the acceleration of the motor side or load side, $\dot{X}$ is the velocity of the motor side or load side, M and L denote the equivalent mass of the linear motor and load mass, respectively. Therefore, this flexible transmission can negatively affect the overall performance in terms of increased vibrations.

1.1 Force estimation

Generally, a force sensor has been widely applied to measure the external force information. However, the bandwidth of the force sensor is not very high since the strain gauge with soft structure is used. Moreover, the information of the force sensor has much noise. Thus, the deterioration of the force sensor is the presence of significant oscillation in the system. Based on the sensorless force control technology, a state observer is used to estimate unknown state variables. Many practical application systems have confirmed that the state observer can be used instead of the real force sensor. However, the exact parameters of the observer are difficult to obtain.

1.1.1 Disturbance observer

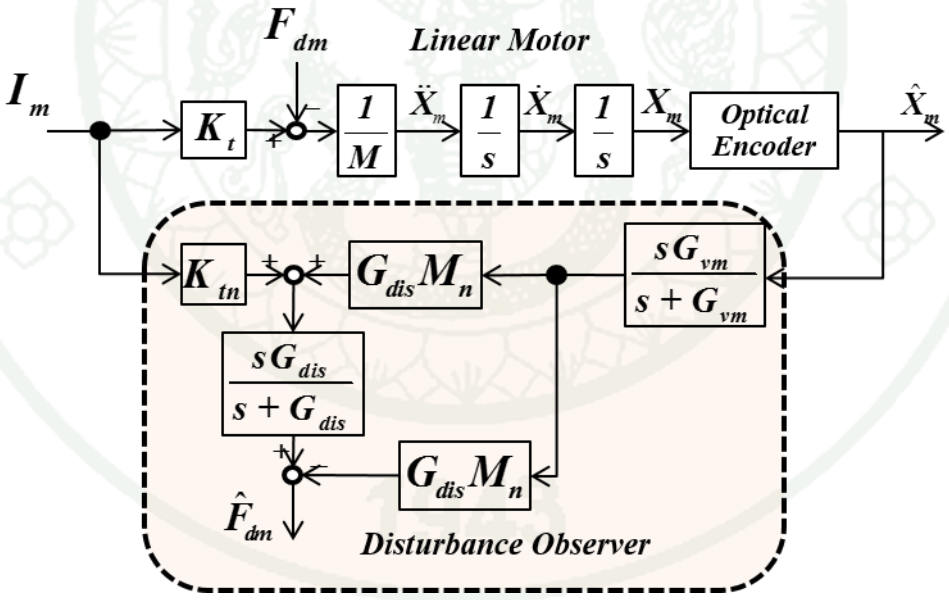

Figure 3 The block digram of disturbance observer.

A disturbance observer (DOB) has become a preferred approach for improving robustness of the force control and accuracy of the force estimation as shown in Figure 3. It has been shown that superior performance with robustness can be achieved by using the DOB. The DOB is simple to design and easy to implement

since a complicated identification of the parameter is not required. The motor current and velocity information is the reference input of the DOB, whereas the external force estimation is the output. It has been confirmed that a robust force control can be obtained, when a disturbance observer is implemented as the feed forward control for a disturbance force compensation loop. Here, the disturbance force on the motor side F_{dm} is defined as

$$F_{dm} = F_{fm} + D_m \dot{X}_m + F_s + \Delta M \ddot{X}_m + \Delta K_t I_m \tag{4}$$

where, the resistive force which the direction is opposite to the motor force is the summation of friction force F_{fm} , viscous friction $D_m \dot{X}_m$ and the spring force F_s. $\Delta M \ddot{X}_m$ is the variation torque due to changed mass, $\Delta K_t I_m$ is the force ripple due to space harmonics. X is the real position but $\hat{X}$ is the measured position from the encoder.

In this thesis, it is assumed that the influence of the friction force is very small by using a small size of linear motor; thus, the spring force has almost the same value of the disturbance estimation algorithm that is based upon motor current and velocity information as shown in

$$\hat{F}_{dm} = \frac{G_{dis}}{s + G_{dis}} (K_{tn} I_m + G_{dis} M_n \hat{\dot{X}}_m) - G_{dis} M_n \hat{\dot{X}}_m \tag{5}$$

$$\hat{\dot{X}}_m = \frac{s G_{vm}}{s + G_{vm}} \hat{X}_m \tag{6}$$

where K_{tn} and M_n are refer to the nominal force coefficient and the nominal motor mass, respectively. G_{dis} is the cut-off frequency of the disturbance observer, G_{vm} is the cut-off frequency of the motor velocity estimation, $\hat{F}_{dm}$ is the estimated disturbance force at the motor side. To apply in the real controller, accurate measured data of velocity is required to provide high accurate force sensing of disturbance observer.

1.1.2 Multi-encoder based on disturbance observer

Because of the advantages and unique features of disturbance observer, this approach has received much attention in sensorless force control system. However, instability and vibration of system can occur when using disturbance observer for the flexible robot system because of the presence of spring that degrade the overall performance. To address these problems, a load disturbance observer (LDOB) is proposed to estimate the external force at the load side. The block diagram of LDOB is shown in Figure 4.

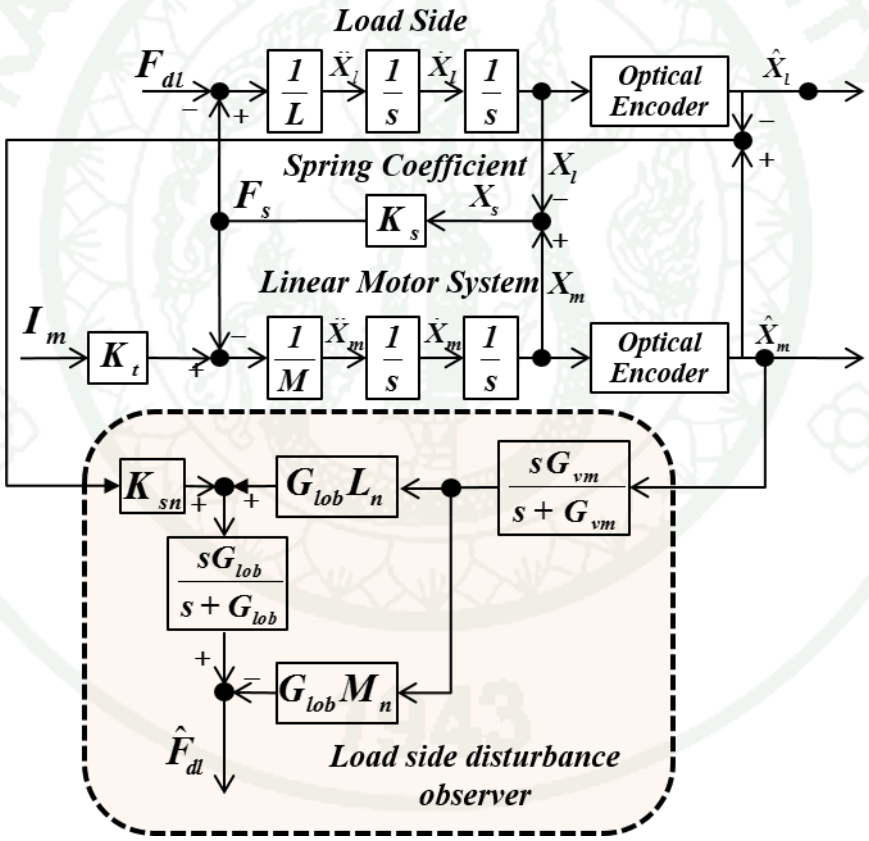

Figure 4 The block diagram of load side disturbance observer.

Here, the disturbance force on the load side F_{dl} is defined as

$$F_{dl} = K_s X_s - L_n \ddot{X}_l \tag{7}$$

$$\hat{F}_{dl} = \left(\frac{G_{lob}}{s + G_{lob}} \left(K_{sn} \left(\hat{X}_l - \hat{X}_m \right) + G_{lob} L_n \hat{\dot{X}}_l \right) - G_{lob} L_n \hat{\dot{X}}_l \right) \tag{8}$$

$$\hat{\dot{X}}_l = \frac{sG_{vm}}{s + G_{vm}} \hat{X}_l \tag{9}$$

where K_{sn} and L_n are refer to the nominal spring coefficient and the nominal load mass, respectively. G_{lob} is the cut-off frequency of the load side disturbance observer, G_{vm} is the cut-off frequency of the motor velocity estimation, $\hat{F}_{dl}$ is the estimated disturbance force at the load side, X_s is the torsional position from the position of the motor X_m and the position of the load X_l. However, the exact parameters of the spring coefficient is difficult to obtain. Moreover, it can be assumed by a non-linear relationship. (Katsura *et al.*, 2006)

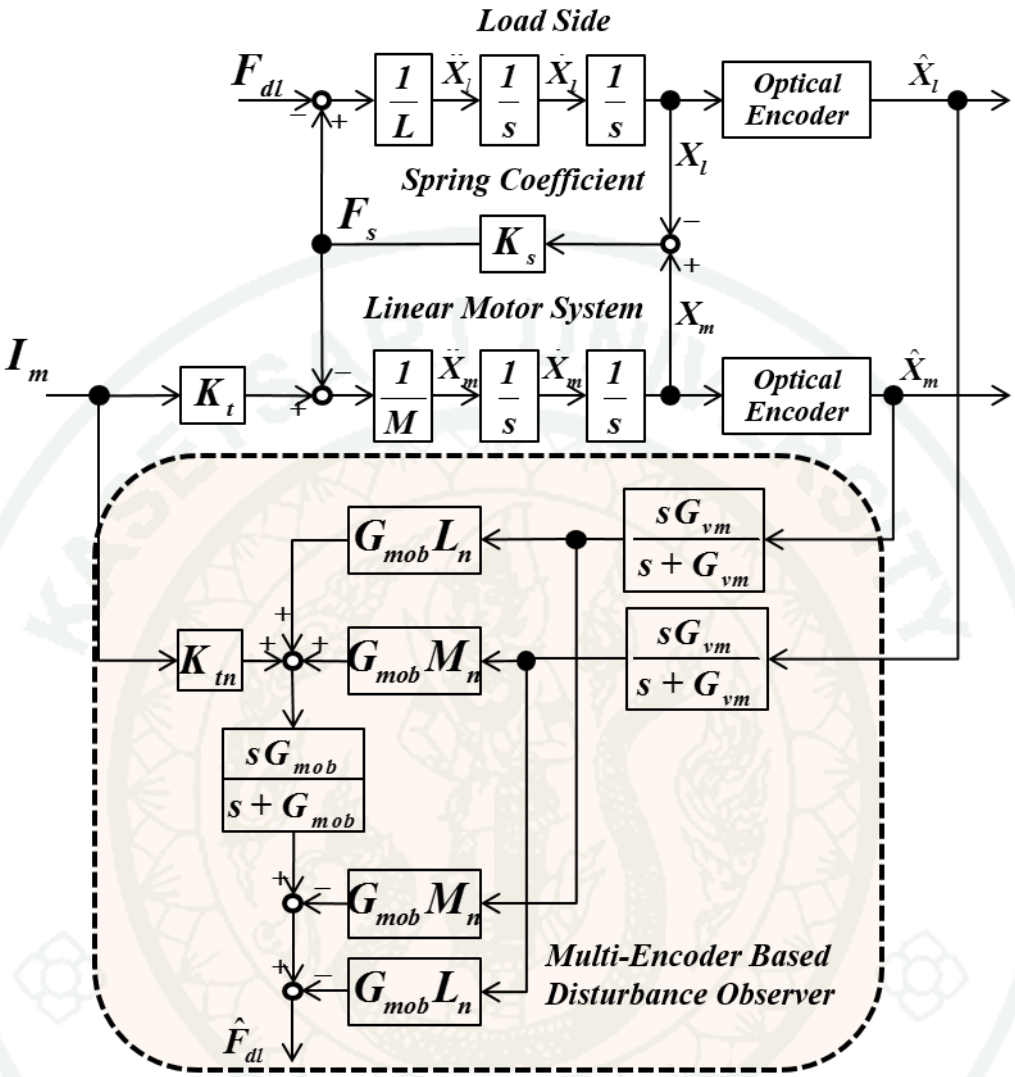

Figure 5 The block diagram of multi-encoder based disturbance observer.

The disturbance force estimation at the load side by LDOB is slowly because the nominal spring coefficient is estimated by a non-linear relationship. A multi encoder-based disturbance observer (MEDOB) is proposed for estimation the external force at the load side of flexible robot as shown in Figure 5. It is not necessary to estimate the nominal spring coefficient parameters. The method to estimate the external force at the load side is obtained from the equation (1), (2) and a simple first-order low-pass filter as follows,

$$F_{dl} = K_{tn} I_m - M_n \ddot{X}_m - L_n \ddot{X}_l \tag{10}$$

$$\hat{F}_{dl} = \left(\frac{G_{mob}}{s + G_{mob}}\left(K_{tn} I_m + G_{mob} M_n \hat{\dot{X}}_m + G_{mob} L_n \hat{\dot{X}}_l\right) - G_{mob} M_n \hat{\dot{X}}_m - G_{mob} L_n \hat{\dot{X}}_l\right) \tag{11}$$

$$\hat{\dot{X}}_m = \frac{sG_{vm}}{s + G_{vm}} \hat{X}_m \tag{12}$$

$$\hat{\dot{X}}_l = \frac{sG_{vm}}{s + G_{vm}} \hat{X}_l \tag{13}$$

where K_{tn}, M_n and L_n are refer to the nominal force coefficient, the nominal mass of motor and the nominal load mass, respectively. G_{mob} is the cut-off frequency of the load side disturbance observer, G_{vm} is the cut-off frequency of the motor velocity estimation, $\hat{F}_{dl}$ is the estimated disturbance force at the load side, X is the real position but $\hat{X}$ is the measured position from the encoder.

Compared to the other conventional ways such as state observer and LDOB, MEDOB offers the advantages of faster response, and high accuracy.

1.2 Force control

Generally, the conventional PID controller is widely used in the industrial machines and robotics. Although this method offers a simple way to design the controller, it does not perform well when the plant system is unstable or has a resonance structural vibration. Therefore, it is necessary to design the controller that guarantees the robustness and suppresses vibration. Controlling machine with the mechanical resonance has been receiving increased attention. A new effective control method, the resonance ratio control has been proposed to improve the robustness and suppress the oscillation during task executions for position control system. This method relies on the possibility to change the virtual inertia moment in the motor side by feeding back the estimated reaction torque to the motor in an acceleration dimension. This means that the resonance frequency and the resonance ratio of the system can be changed to an arbitrarily value.

In this thesis, the resonance ratio control is used to control the force for suppressing the vibration of the system. In addition, the control parameter can design for the good performance by using the CDM.

1.2.1 Resonance ratio control

The simplified block diagram of this reaction force feedback is shown in Figure 6. The controller of robot system consist of a force gain K_p , a velocity gain K_v and a reaction force gain K_r. The feedback force will depend on the force contacted on the robot by a known environment stiffness K_e.

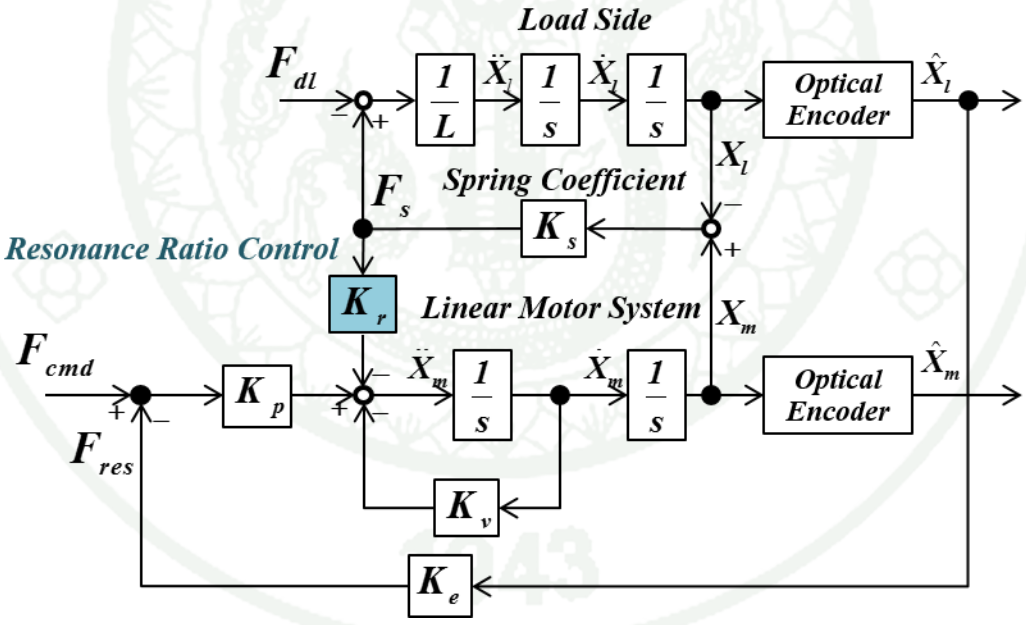

Figure 6 The simplified block diagram of the resonance ratio control in the two-mass system.

From Figure 6, the transfer functions from acceleration reference $\ddot{X}_{ref}$ to motor position $\hat{X}_m$ and motor position $\hat{X}_m$ to load position $\hat{X}_l$ can be calculated as follows,

$$\frac{\hat{X}_m}{\ddot{X}_{ref}} = \frac{Ls^2 + K_s}{Ls^4 + K_s(1 + \mathrm{K}_r\mathrm{L})\mathrm{s}^2} \tag{14}$$

$$\frac{\hat{X}_l}{\hat{X}_m} = \frac{K_s}{Ls^2 + K_s} \tag{15}$$

Such a reaction force feedback is able to change the resonance frequency of the system. The resonance frequency of the motor side ω_r and the anti-resonance frequency of the load side ω_{ar} can be computed as follows,

$$\omega_r = \sqrt{\frac{K_s}{L}(1 + K_r L)} \tag{16}$$

$$\omega_{ar} = \sqrt{\frac{K_s}{L}} \tag{17}$$

The transfer function of the force servo based on resonance ratio control is given by

$$\frac{F_{res}}{F_{cmd}} = \frac{K_p K_e \omega_{ar}^2}{s^4 + K_v s^3 + \omega_r^2 s^2 + K_v \omega_{ar}^2 s + K_p K_e \omega_{ar}^2} \tag{18}$$

1.2.2 Coefficient diagram method

The resonance ratio control must be the optimum parameters for the best performance, which design by the coefficient diagram method. CDM is used to design the characteristic polynomial of the close loop system by achieving a good balance of stability and good robust performance. As it is seen from equation (18), the coefficients of characteristic polynomial a_i are found as

$$a_0 = K_p K_e \omega_{ar}^2 \tag{19}$$

$$a_1 = K_v \omega_{ar}^2 \tag{20}$$

$$a_2 = \omega_r^2 \tag{21}$$

$$a_3 = K_v \tag{22}$$

$$a_4 = 1 \tag{23}$$

The standard stability indices γ_i for the Manabe form are chosen as $\gamma_1 = 2.5$, $\gamma_2 = 2.0$, and $\gamma_3 = 2.0$. The equations calculated between a_i and γ_i as follow

$$\tau = \frac{a_1}{a_0} = \frac{K_v}{K_p K_e} \tag{24}$$

$$\gamma_1 = \frac{a_1^2}{a_0 a_2} = \frac{K_v^2 \omega_{ar}^2}{K_p K_e \omega_r^2} = 2.5 \tag{25}$$

$$\gamma_2 = \frac{a_2^2}{a_1 a_3} = \frac{\omega_r^4}{K_v^2 \omega_{ar}^2} = 2.0 \tag{26}$$

$$\gamma_3 = \frac{a_3^2}{a_2 a_4} = \frac{K_v^2}{\omega_r^2} = 2.0 \tag{27}$$

Thus, the controller parameters calculated by the design of CDM are given as follows

$$K_v = \sqrt{2}\omega_r \tag{28}$$

$$K_p = \frac{4\omega_{ar}^2}{5K_e} \tag{29}$$

$$K = \frac{\omega_r}{\omega_{ar}} = 2.0 \tag{30}$$

$$K_r = \frac{3}{L_1} \tag{31}$$

1.2.3 Feedforward load disturbance compensation

The block diagram of the closed-loop resonance ratio control can be seen in Figure 7. A robust motion control of each motor has been achieved by feedback the inner disturbance observer loop. By using the divider's gain $1/K_{tn}$, the disturbance force is transformed to the compensation current $\hat{I}_{dis}$, and it is utilized to cancel out the disturbance on the motor side and the uncertainly of a system due to the parameter variation. In addition, the external force on the load side is the force from impedance model, which is used to generate the disturbance force at the second load side, which is represented as follow:

$$F_{env} = \left(K_{ss} + K_{dd}s\right)X_l \tag{32}$$

where F_{env} is the reaction force from the environments, K_{ss} and K_{dd} are the spring coefficient and the damper coefficient.

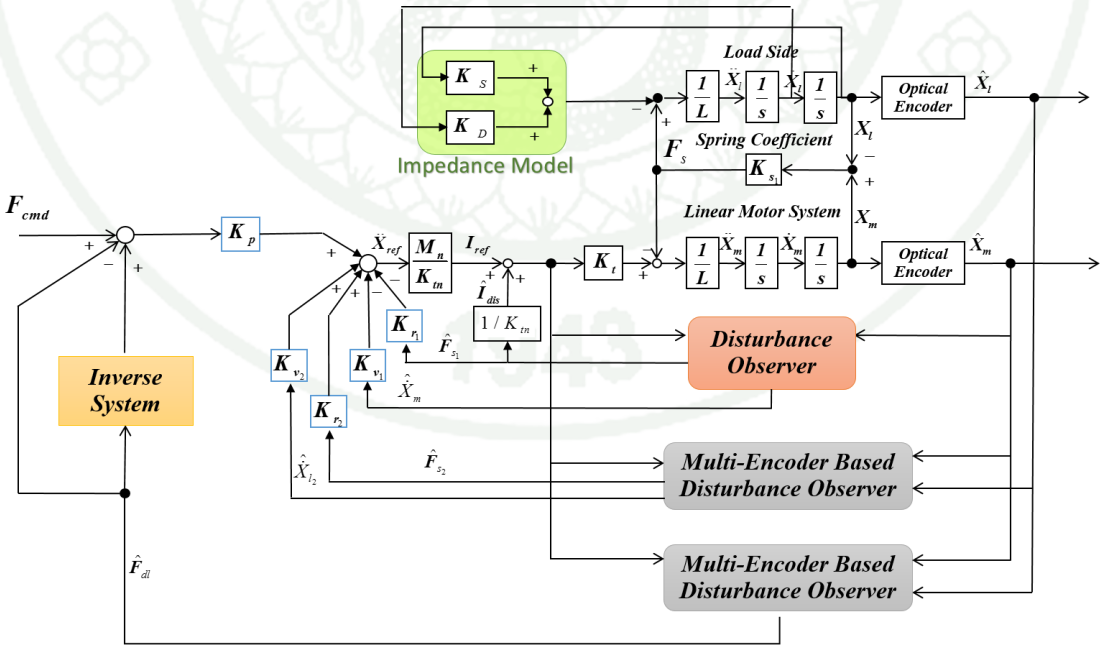

Figure 7 The resonance ratio control based on MEDOB and CDM in the two-mass system.

The load disturbance compensation is introduced to compute and feedback the estimated load disturbance force through the inverse system of the motor side. The inverse system can be represented by the transfer function from F_{cmd} to F_{res} as shown in (18) and from F_{dl} to F_{res} as follows

$$\frac{F_{res}}{F_{dl}} = \frac{\frac{1}{L}K_e(\mathrm{s}^2 + \mathrm{K}_v\mathrm{s} + \mathrm{K}_r\mathrm{K}_s)}{s^4 + K_v s^3 + \omega_r^2 s^2 + K_v\omega_{ar}^2 s + K_p K_e \omega_{ar}^2} \tag{33}$$

Then, the inverse system can be calculated by the following equation

$$\frac{F_{cmd}}{F_{dl}} = \frac{\mathrm{s}^2 + \mathrm{K}_v\mathrm{s} + \mathrm{K}_r\mathrm{K}_s}{K_p K_s} \tag{34}$$

2. Three - mass system

The model of the three-mass system has the same structure as the two-mass system, but the three-mass system has two load mass. Therefore, the three-mass system consist of a motor M and a load L_1, L_2 connected by a flexible structure to transmit the actuator torque to a distant joint. Therefore, the elasticity of flexible robot is realized under assumptions that it can be modeled by constant spring coefficient K_{s_1}, K_{s_2} and mass system as shown in Figure 8. Where K_{s_1} is the flexible connecter between the motor and the first load and K_{s_2} is the flexible connecter between the first load and the second load.

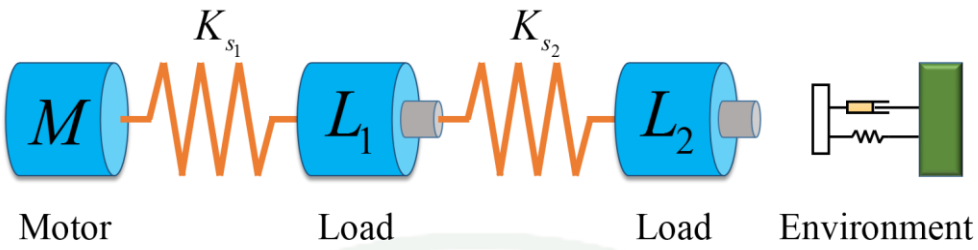

Figure 8 The model of the three-mass system.

A block diagram of the motor with the three-mass system that controls under the ideal current source is shown in Figure 9. The dynamic equation of the linear motor can be described by:

$$\ddot{X}_m = -\frac{K_{s_1}}{M} X_{s_1} + \frac{K_t}{M} I_m \tag{35}$$

$$\ddot{X}_{l_1} = \frac{K_{s1}}{L_1} X_{s_1} - \frac{K_{s_2}}{L_2} X_{s_2} \tag{36}$$

$$\ddot{X}_{l_2} = \frac{K_{s_2}}{L_2} X_{s_2} - \frac{1}{L_2} F_{dl_2} \tag{37}$$

$$\dot{X}_{s_1} = \dot{X}_m - \dot{X}_{l_1} \tag{38}$$

$$\dot{X}_{s_2} = \dot{X}_{l_1} - \dot{X}_{l_2} \tag{39}$$

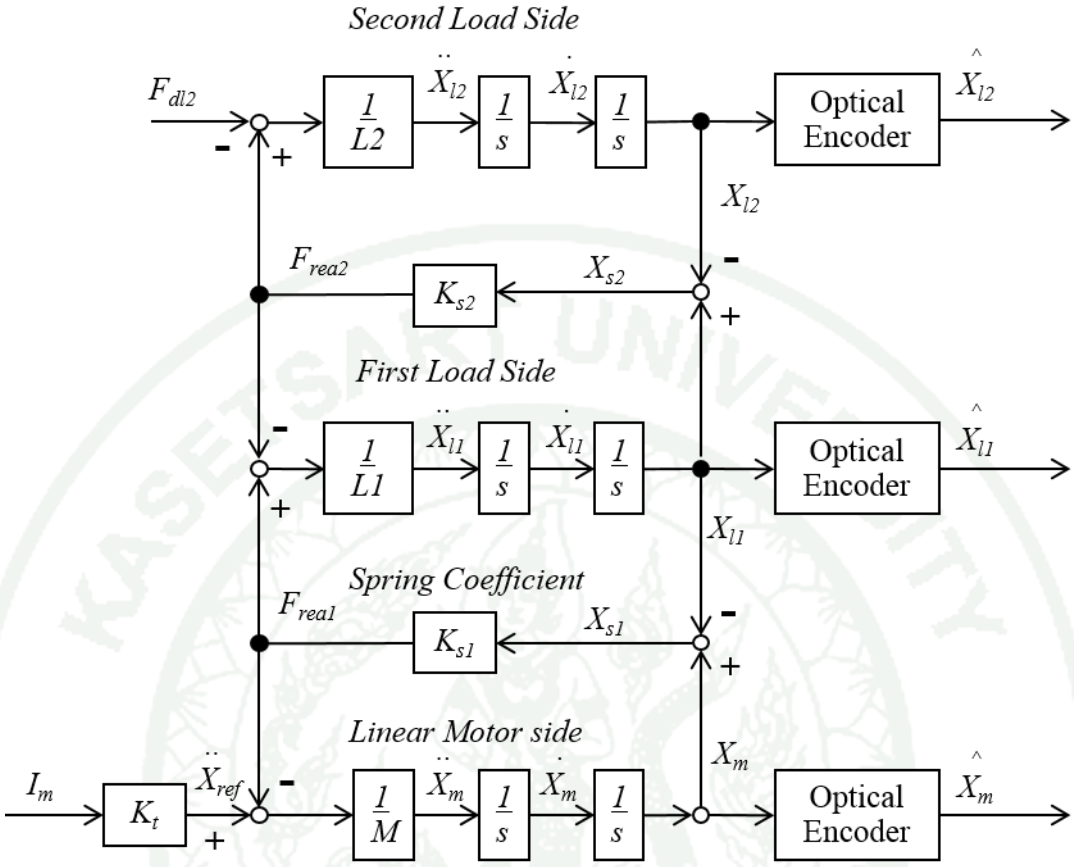

Figure 9 The block diagram of the three-mass system.

From Figure 9, the transfer functions from acceleration reference $\ddot{X}_{ref}$ to motor position $\hat{X}_m$, motor position $\hat{X}_m$ to first load position $\hat{X}_{l_1}$ and first load position $\hat{X}_{l_1}$ to second load position $\hat{X}_{l_2}$,can be calculated as follows,

$$\frac{\hat{X}_{l_2}}{X_{l1}} = \frac{K_{s_2}}{\left(L_2 s^2 + K_{s_2}\right)} \tag{40}$$

$$\frac{\hat{X}_{l_1}}{\hat{X}_m} = \frac{K_{s_1}\left(L_2 s^2 + K_{s_2}\right)}{L_1 L_2 s^4 + \left(K_{s_1} L_2 + K_{s_2} L_1 + K_{s_2} L_2\right) s^2 + K_{s_1} K_{s_2}} \tag{41}$$

$$\frac{\hat{X}_m}{\ddot{X}_{ref}} = \frac{L_1 L_2 s^4 + \left(K_{s_1} L_2 + K_{s_2}\left(L_1 + L_2\right)\right) s^2 + K_{s_1} K_{s_2}}{L_1 L_2 M s^6 + \left(K_{s_1}\left(L_1 L_2 + L_2 M\right) + K_{s_2} M\left(L_1 + L_2\right)\right) s^4 + \left(K_{s_1} K_{s_2}\left(L_1 + L_2 + M\right)\right) s^2} \tag{42}$$

Where subscripts m, l_1 and l_2 denote the motor side, the first load side and the second load side, respectively. F_{s_1}, F_{s_2} and F_{dl_2} are the first spring force, the second spring force and the external force on the load side. K_t is the force coefficient, I_m is the current, X_{s_1} is the torsional position from the position of the motor X_m and the position of the load X_{l_1}, X_{s_2} is the torsional position from the position of the motor X_{l_1} and the position of the load X_{l_2}, M and L denote the equivalent mass of the linear motor and load mass, respectively. Therefore, there is more vibrations in the three-mass system than in the two-mass system.

2.1 Force estimation

In the three – mass system, MEDOB is used to estimate the external force on the second load side. DOB is used to estimate the external force on the motor side for compensate the disturbance and uncertainly of the system due to the internal parameters change as same as the two – mass system.

2.1.1 Multi-encoder based on disturbance observer

MEDOB is used to estimate the external force on the second load side in the three – mass system as shown in Figure 10. The equations show mathematic calculation for estimate the external force as follow

$$F_{dl} = K_t I_m - L_1 \ddot{X}_{l_1} - L_2 \ddot{X}_{l_2} - M\ddot{X}_m \tag{43}$$

$$\hat{F}_{dl} = \frac{G_{mob}}{s + G_{mob}}(K_{tn} I_m + G_{mob} M_n \hat{\dot{X}}_m + G_{mob} L_1 \hat{\dot{X}}_{l_1} + G_{mob} L_2 \hat{\dot{X}}_{l_2})$$

$$-G_{mob} L_{1n} \hat{\dot{X}}_{l_1} - G_{mob} L_{2n} \hat{\dot{X}}_{l_2} - G_{mob} M_n \hat{\dot{X}}_m \tag{44}$$

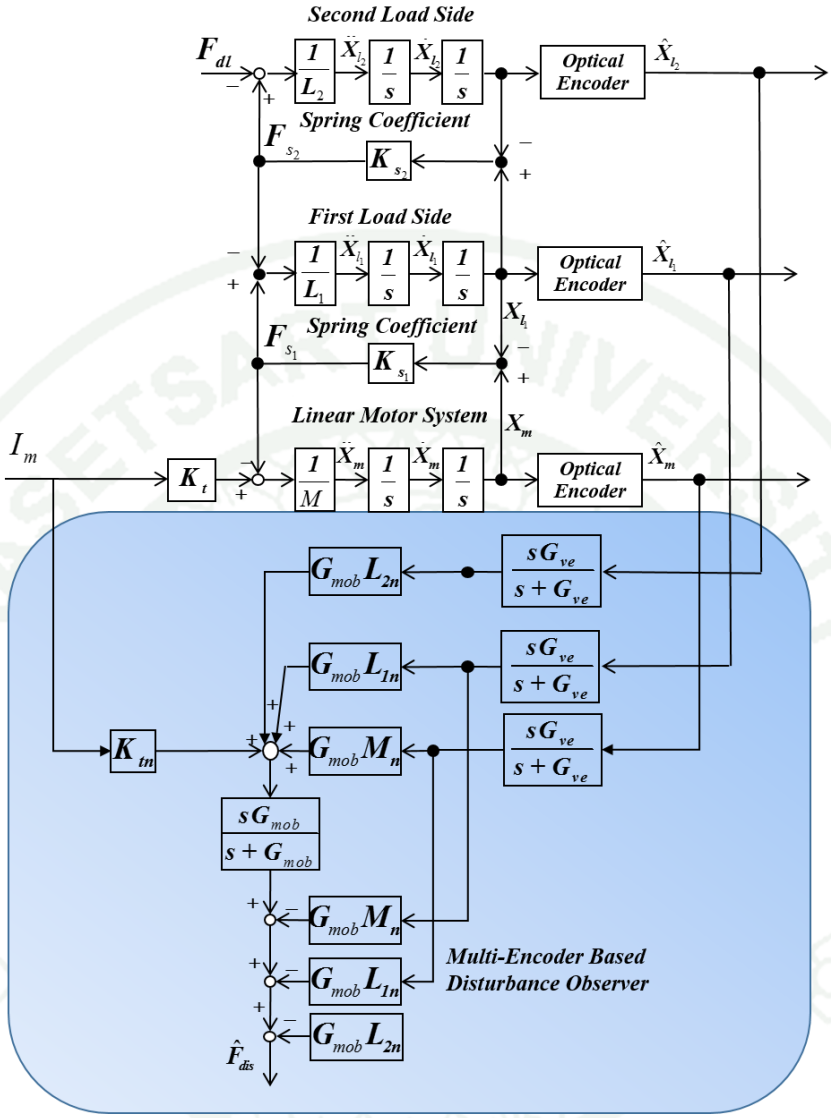

Figure 10 The block diagram of multi-encoder based disturbance observer

2.2 Force control

In this thesis, the vibration is occurred by using the conventional PID controller. Therefore, the resonance ratio control is used to control force because it has ability to improve the robust when the system has a disturbance or vibration from the flexible structure.

2.2.1 Resonance ratio control

The simplified block diagram of this reaction force feedback is shown in Figure 11. The controller of robot system consists of a force gain K_p , two velocity gains K_{v_1}, K_{v_2} and two reaction force gains K_{r_1}, K_{v_2}. The feedback force will depend on the force contacted on the robot by a known environment stiffness K_e.

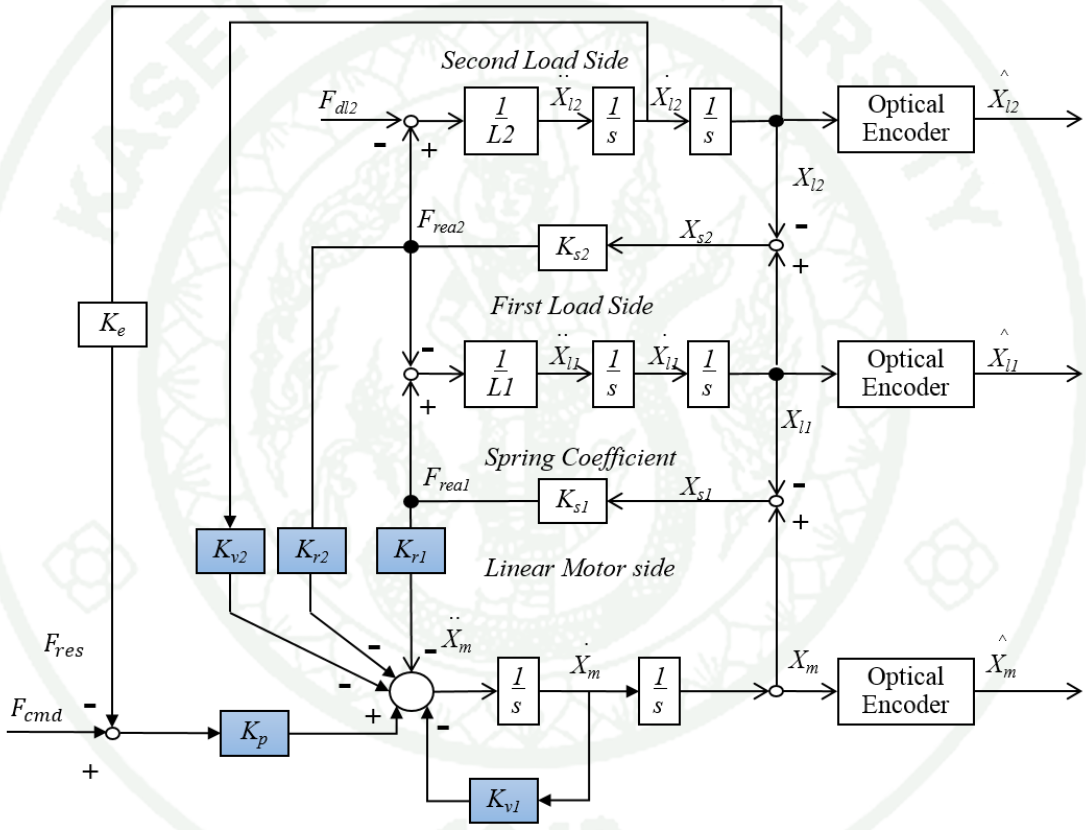

Figure 11 The simplified block diagram of the resonance ratio control in the three - mass system.

From Figure 11, the transfer functions from acceleration reference $\ddot{X}_{ref}$ to motor position $\hat{X}_m$, motor position $\hat{X}_m$ to first load position $\hat{X}_{l_1}$ and first load position $\hat{X}_{l_1}$ to second load position $\hat{X}_{l_2}$,can be calculated as follows,

$$\frac{\hat{X}_{l_2}}{X_{l1}} = \frac{K_{s_2}}{\left(L_2 s^2 + K_{s_2}\right)} \tag{45}$$

$$\frac{\hat{X}_{l_1}}{\hat{X}_m} = \frac{K_{s_1}\left(L_2 s^2 + K_{s_2}\right)}{L_1 L_2 s^4 + \left(K_{s_1} L_2 + K_{s_2} L_1 + K_{s_2} L_2\right) s^2 + K_{s_1} K_{s_2}} \tag{46}$$

$$\frac{\hat{X}_m}{\ddot{X}_{ref}} = \frac{L_1 L_2 s^4 + \left(K_{s_1} L_2 + K_{s_2} L_1 + K_{s_2} L_2\right) s^2 + K_{s_1} K_{s_2}}{c_6 s^6 + c_5 s^5 + c_4 s^4 + c_3 s^3 + c_2 s^2 + c_1 s} \tag{47}$$

$$c_1 = K_{s_1} K_{s_2}\left(K_{v_1} + K_{v_2}\right) \tag{48}$$

$$c_2 = K_{s_1} K_{s_2}\left(1 + K_{r_1}\left(L_1 + L_2\right) + K_{r_2} L_2\right) \tag{49}$$

$$c_3 = K_{s_1} K_{v_1} L_2 + K_{s_2} K_{v_1}\left(L_1 + L_2\right) \tag{50}$$

$$c_4 = K_{s_1} L_2 + K_{s_2} L_1 + K_{s_2} L_2 + K_{r_1} K_{s_1} L_1 L_2 \tag{51}$$

$$c_5 = K_{v_1} L_1 L_2 \tag{52}$$

$$c_6 = L_1 L_2 \tag{53}$$

From the equation(47), K_{r1}, K_{r2}, K_{v1}, and K_{v2} have affected in characteristic equation of the transfer function. This means that the resonance frequency of the system can be changed to an arbitrarily value which it extends bandwidth for better control of higher frequency input as shown in the results. From Figure 11, the transfer functions from the force command F_{cmd} to the force response F_{res} can be calculated as follows,

$$\frac{F_{res}}{F_{cmd}} = \frac{K_e K_p K_{s_1} K_{s_2}}{a_6 s^6 + a_5 s^5 + a_4 s^4 + a_3 s^3 + a_2 s^2 + a_1 s + a_0} \tag{54}$$

$$a_0 = K_e K_p K_{s_1} K_{s_2} \tag{55}$$

$$a_1 = K_{s_1} K_{s_2}\left(K_{v_1} + K_{v_2}\right) \tag{56}$$

$$a_2 = K_{s_1} K_{s_2}\left(1 + L_1 + L_2\right) + K_{s_1} K_{s_2}\left(K_{r_1} L_1 + K_{r_2} L_2\right) \tag{57}$$

$$a_3 = K_{s_1} K_{v_1} L_2 + K_{s_2} K_{v_1}\left(L_1 + L_2\right) \tag{58}$$

$$a_4 = K_{s_1} L_2 + K_{s_2} \left(L_1 + L_2 \right) + \left(K_{s_1} + K_{r_1} K_{s_1} \right) L_1 L_2 \tag{59}$$

$$a_5 = K_{v_1} L_1 L_2 \tag{60}$$

$$a_6 = L_1 L_2 \tag{61}$$

2.2.2 Coefficient diagram method (CDM)

Like the two-mass system, CDM is also used to design the characteristic polynomial of the closed loop system by achieving a good balance of stability and good robust performance. As it can be seen from equation(54), the coefficients of characteristic polynomial a_i are found as in equation(55)-(61).

The standard stability indices γ_i for the Manabe form are chosen as $\gamma_1 = 2.5$, $\gamma_2 = 2.0$, $\gamma_3 = 2.0$, $\gamma_4 = 2.0$ and $\gamma_5 = 2.0$.(Shunji, M., 1998) The equations show the calculation between a_i and γ_i as follow:

$$\tau = \frac{a_1}{a_0} = \frac{K_v}{K_p K_e} \tag{62}$$

$$\gamma_1 = \frac{a_1^2}{a_0 a_2} = 2.5 \tag{63}$$

$$\gamma_2 = \frac{a_2^2}{a_1 a_3} = 2.0 \tag{64}$$

$$\gamma_3 = \frac{a_3^2}{a_2 a_4} = 2.0 \tag{65}$$

$$\gamma_4 = \frac{a_4^2}{a_3 a_5} = 2.0 \tag{66}$$

$$\gamma_5 = \frac{a_5^2}{a_4 a_6} = 2.0 \tag{67}$$

Thus, the controller parameters calculated by the design of CDM like in the two-mass system.

2.2.3 Feedforward load disturbance compensation

The block diagram of the closed-loop resonance ratio control can be seen in Figure 12. A robust motion control of each motor can be achieved by feedback the inner disturbance observer loop. By using the divider's gain $1/K_{tn}$, the disturbance force is transformed to the compensation current $\hat{I}_{dis}$, and it is utilized to cancel out the disturbance on the motor side and the uncertainly of a system due to the parameter variation. In addition, the external force on the load side is the force from impedance model (32).

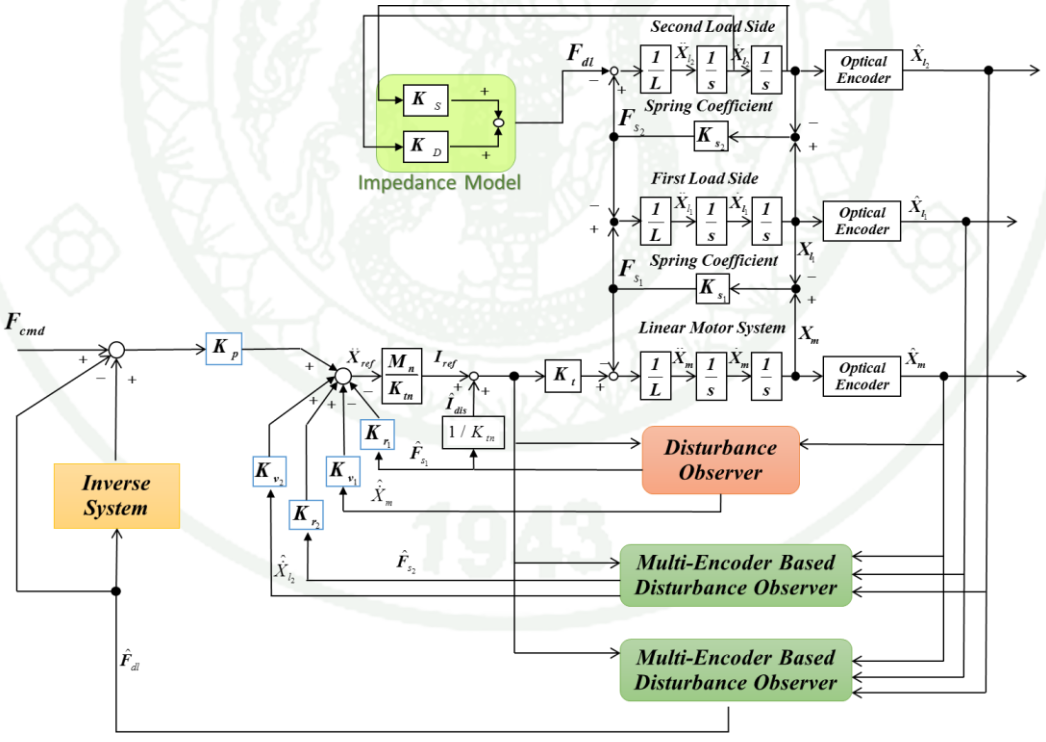

Figure 12 The block diagram of resonance ratio control based on MEDOB and CDM in the three-mass system.

The load disturbance compensation is introduced to compute and feedback the estimated load disturbance force through the inverse system of the motor side. The inverse system can be represented by the transfer function from F_{cmd} to F_{res} as shown in (54) and from F_{dl} to F_{res} as follows

$$\frac{F_{res}}{F_{dl}} = \frac{K_e\left(L_1 s^4 + K_{v_1} L_1 s^3 + \left(K_{s_1} + K_{s_2} + K_{r_1} K_{s_1} L_1\right)s^2 + \left(K_{s_1} + K_{s_2}\right)K_{v_1}\,s + \left(K_{r_1} + K_{r_2}\right)K_{s_1} K_{s_2}\right)}{a_6 s^6 + a_5 s^5 + a_4 s^4 + a_3 s^3 + a_2 s^2 + a_1 s + a_0} \quad (68)$$

Then, the inverse system can be calculated by the following equation:

$$\frac{F_{cmd}}{F_{dl}} = \frac{L_1 s^4 + K_{v_1} L_1 s^3 + \left(K_{s_1} + K_{s_2} + K_{r_1} K_{s_1} L_1\right)s^2 + \left(K_{s_1} + K_{s_2}\right)K_{v_1}\,s + \left(K_{r_1} + K_{r_2}\right)K_{s_1} K_{s_2}}{K_p K_{s_1} K_{s_2}} \quad (69)$$

3. Bilateral control

Control of master-slave robots working in bilateral control has been a challenging research in this area in recent years. Robots in the master-slave configurations have been proposed to perform tasks in many application areas. The bilateral control supplies force feedback information to the human operator through a master robot. On the other hand, a slave robot applies to interact with unknown environments. Both of master and slave robots are bilaterally controlled with the same actions of force and motion movements. In the bilateral control, the same sensor units and the structure of the mechanics are generally used. In order to make the robot system more efficient, flexible, and applicable, the different types of motor and sensor need to be designed and constructed. For example, the robot arm on the mobile robot is controlled to operate the complex tasks by a joystick at the master side. This way, the robot arm on the mobile robot at the slave side is used to interact with and operate in an open environment.

3.1 Concept of the bilateral control

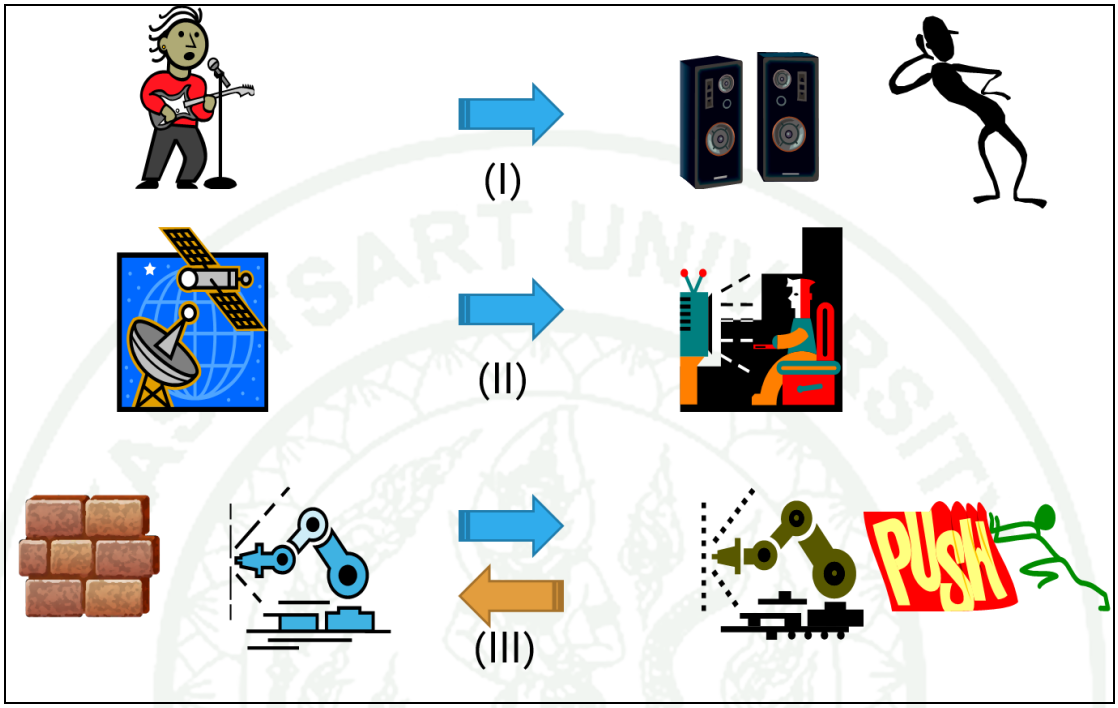

Figure 13 The data transmission.

Multimedia technologies are used widely today because of their advantages to transform and record experience information in a purposeful way as shown in Figure 13. First as seen in I, a microphone is used for converting and recording sound into an electrical signal. Then, the electrical signal must be reconverted to analog form during playback before it is applied to a speaker. Second as seen in II, the video is obtained by a video camera. By using a television or monitor, it is possible to transmit visual sensation via the broadcasting channel. However, such information is always transfer in only one-way direction. Third as seen in III, the human pushes the master robot in the right side to move and the slave robot follow too. Moreover, when the slave robot touches the rock in the left side, it must transmit the reaction force to the human at the master side to be better control the master slave robot. However, such information is always transfer in round direction.

To provide the sense of touch, robots in master-slave configurations have been proposed. The exchanged information between motors is base on the concept of the bilateral control. The bilateral control supplies force feedback information to the human operator through a master robot. On the other hand, a slave robot is applied to interact with unknown environments.

The bilateral control is the bidirectional control of force and position based on the Newton's law of action and reaction. The complexities that control the master-slave robots present are synchronized in terms of movements and force. Master and slave robots must be controlled similarly. Thus, the target of the ideal bilateral control is to minimize the difference between the force responses in the master side $\hat{F}_{ext}^{m}$ and slave side $\hat{F}_{ext}^{s}$ as follows:

$$\hat{F}_{ext}^{m} = -\hat{F}_{ext}^{s} \tag{70}$$

$$\hat{F}_{ext}^{m} + \hat{F}_{ext}^{s} = 0 \tag{71}$$

Moreover, the position tracking of the master robot $\hat{X}_{m}^{m}$ and slave robot $\hat{X}_{m}^{s}$ should be similar, as follows

$$\hat{X}_{m}^{m} = \hat{X}_{m}^{s} \tag{72}$$

$$\hat{X}_{m}^{m} - \hat{X}_{m}^{s} = 0 \tag{73}$$

Generally, a DOB with the same optical encoder has been implemented to estimate force sensation in the bilateral control system as shown in (Natori, K. *et al.*, 2010;Yokokura, Y. *et al.*, 2009). In multi-mass system, the DOB cannot estimate the external force at load side. Thus, using the MEDOB instead.

3.2 Control Mode

From the concept of bilateral control, the force control is worked together with the position control. Therefore, it has two control modes, namely; the common mode and differential mode, are implemented and applied to control both the position and force. In order to obtain information for the modal space design, the force estimations from the MEDOB at the master side $\hat{F}_{ext}^{m}$ and the slave side $\hat{F}_{ext}^{m}$ are transformed into the virtual force in the common mode $\hat{F}_{ext}^{c}$ and the differential mode $\hat{F}_{ext}^{d}$ by using the second-order Hadamard matrix H_2. On the other hand, the position signals from the optical linear encoder at the master side $\hat{X}_{l}^{m}$ and at the slave side $\hat{X}_{l}^{s}$ are also transformed into the virtual positions in the common mode $\hat{X}_{l}^{c}$ and the differential mode $\hat{X}_{l}^{d}$ by using H_2. The virtual position and force of each mode are represented as follows

$$\begin{bmatrix} \hat{F}_{ext}^{c} \\ \hat{F}_{ext}^{d} \end{bmatrix} = \begin{bmatrix} 1 & 1 \\ 1 & -1 \end{bmatrix} \begin{bmatrix} \hat{F}_{ext}^{m} \\ \hat{F}_{ext}^{s} \end{bmatrix} = H_2 \begin{bmatrix} \hat{F}_{ext}^{m} \\ \hat{F}_{ext}^{s} \end{bmatrix} \tag{74}$$

$$\begin{bmatrix} \hat{X}_{l}^{c} \\ \hat{X}_{l}^{d} \end{bmatrix} = \begin{bmatrix} 1 & 1 \\ 1 & -1 \end{bmatrix} \begin{bmatrix} \hat{X}_{l}^{m} \\ \hat{X}_{l}^{s} \end{bmatrix} = H_2 \begin{bmatrix} \hat{X}_{l}^{m} \\ \hat{X}_{l}^{s} \end{bmatrix} \tag{75}$$

The force control in the common mode can be separately analyzed as the proportional controller. On the other hand, the position control in the differential mode can be analyzed as the proportional – derivative controller. The modal space design of each mode is controlled in the acceleration dimension as shown in the following equations:

$$\ddot{X}_{ref}^{c} = (\mathrm{F}_{cmd}^{c} - \mathrm{F}_{ext}^{c})\,\mathrm{K}_{f} \tag{76}$$

$$\ddot{X}_{ref}^{d} = (\mathrm{X}_{cmd}^{d} - \hat{X}_{l}^{d})(\mathrm{K}_{p} + \mathrm{sK}_{d}) \tag{77}$$

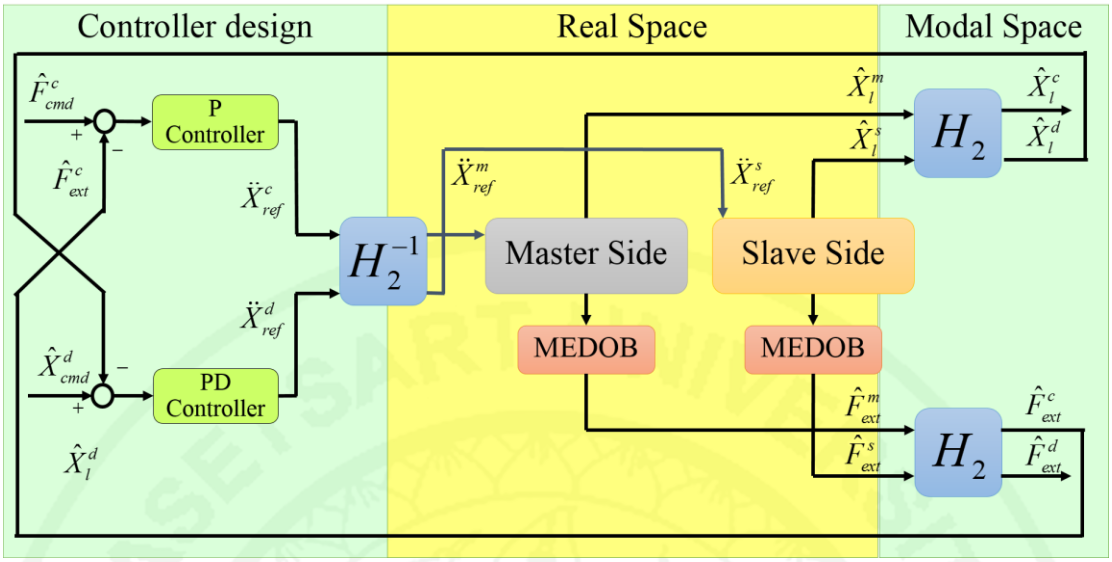

Figure 14 The block digram of the bilaeral control.

where F^c_{cmd} is the force command and X^d_{cmd} is the position command. According to the targets of the bilateral control, both force and position commands were set as zero. K_f is the proportional gain of force control. K_p and K_d are the proportional gain and the derivative gain of position control, respectively.

In order to transform into the master and slave robots, the H_2^{-1} matrix is applied. The transformation of acceleration control signal from the modal space to the real space in the master and slave robots is calculated as follows

$$\begin{bmatrix} \ddot{X}^m_{ref} \\ \ddot{X}^s_{ref} \end{bmatrix} = \frac{1}{2}\begin{bmatrix} 1 & 1 \\ 1 & -1 \end{bmatrix}\begin{bmatrix} \ddot{X}^c_{ref} \\ \ddot{X}^d_{ref} \end{bmatrix} = H_2 \begin{bmatrix} \ddot{X}^c_{ref} \\ \ddot{X}^d_{ref} \end{bmatrix} \tag{78}$$

where $\ddot{X}^c_{ref}$ and $\ddot{X}^d_{ref}$ are the acceleration control signals in the common and differential modes, respectively. $\ddot{X}^m_{ref}$ and $\ddot{X}^s_{ref}$ are the acceleration control signals at the master and slave sides, respectively. The block diagram of bilateral control is shown in Figure 14. However, the problem of flexible robot system, such as

undesirable oscillations and instability, does degrade the performance not only at the slave side but also at the whole system. In order to develop the bilateral control, the method to control a robot in contact with an unknown environment is desired strongly.

4. Simulations

In this thesis, MATLAB and Simulink implement the simulations. The block diagram and the parameter are as follow:

4.1 Two - mass system

In two - mass system, the parameters must be configured before running the simulation which are defined the values of parameters in the m-file. The parameters used in the simulations are shown in Table 1.

4.1.1 Force estimation

The block diagram of DOB and MEDOB in the Simulink are shown in Figure 15 and Figure 16, respectively.

Table 1 The parameters used in simulations of the two-mass system

Details	Parameters	Values
Mass of motor	M	0.245 (kg)
Mass of load	L	0.245 (kg)
Force constant	K_t	3.333
Environment stiffness	K_e	1100
Spring coefficient	K_s	1100 (N/m)
Cut-off freq. of velocity	G_{ve}	1000 (rad/s)

Table 1 (Continued)

Details	Parameters	Values
Cut-off freq. of DOB	G_{dis}	1000 (rad/s)
Cut-off freq. of MEDOB	G_{mob}	800 (rad/s)
Force gain	K_p	3.59
Reaction force gain	K_r	12.24
Velocity gain	K_v	189.52

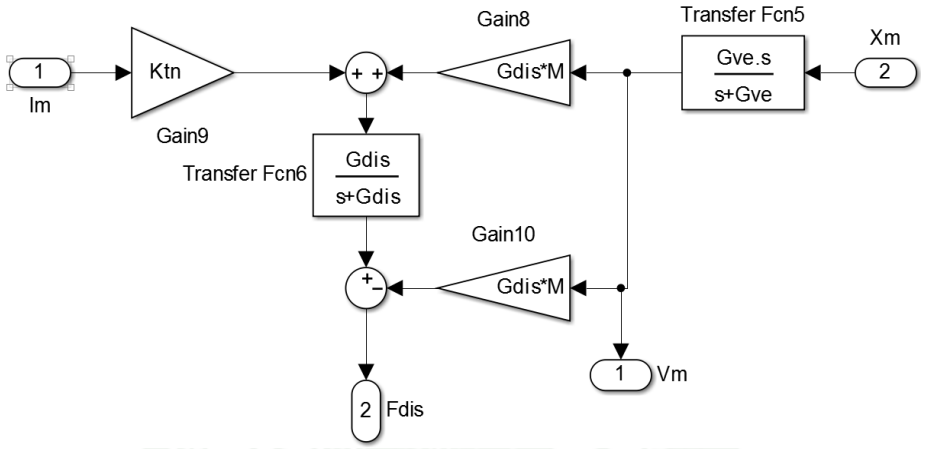

Figure 15 The block diagram of DOB in the simulink.

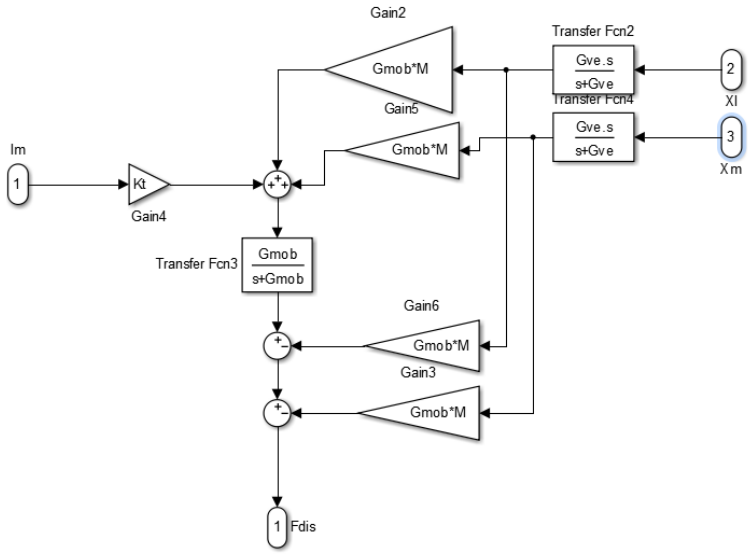

Figure 16 The block diagram of MEDOB for the two-mass system in the simulink.

4.1.2 Force control

The block diagram of the resonance ratio control with MEDOB in the Simulink is shown in Figure 17. In addition, the external force on the load side is the force from impedance model (32).

The optimum parameters are designed by CDM. They can calculated in MATLAB. Firstly, the configuration a_i are equal to the coefficients of characteristic polynomial. Then, the parameters are calculated by CDM with the standard stability indices of Manabe. The source code of design are shown in Figure 18.

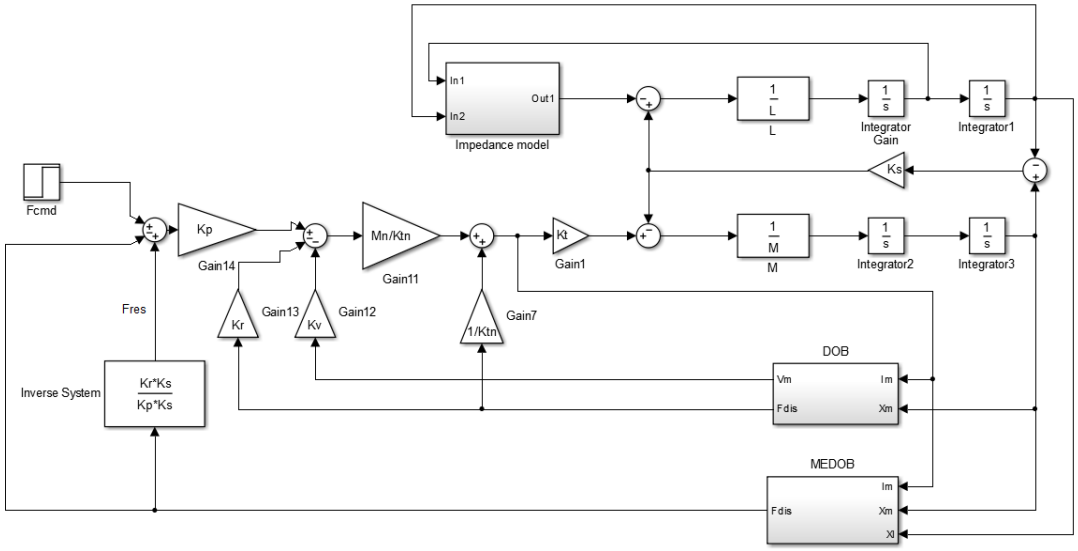

Figure 17 The block diagram of resonance ratio control with MEDOB for the two - mass system.

Define the parameters

```
a0=Ke*Kp*War^2;
a1=Kv*War^2;
a2=Wr^2;
a3=Kv;
a4=1;
```

Calculation

```
t=a1/a0;
g1=(a1^2/(a2*a0));
g2=(a2^2/(a3*a1));
g3=(a3^2/(a4*a2));
[Kp Kr Kv] = solve(g1 == 2.5, g2 == 2, g3 ==2,Kp,Kr,Kv)
```

Figure 18 The design code of CDM in the two-mass system.

4.2 Three - mass system

In three-mass system, the parameters must be configured before run the simulation which are defined the values of parameters in the m-file same the two - mass system. The parameters used in the simulations are shown in Table 2.

Table 2 The parameters used in simulations of the three-mass system

Details	Parameters	Values
Mass of motor	M	0.245 (kg)
Mass of load	L_1, L_2	0.245 (kg)
Force constant	K_t	3.333
Environment stiffness	K_e	11
Spring coefficient	K_{s_1}, K_{s_2}	200, 220 (N/m)
Cut-off freq. of velocity	G_{ve}	250 (rad/s)
Cut-off freq. of DOB	G_{dis}	250 (rad/s)
Cut-off freq. of MEDOB	G_{mob}	250 (rad/s)
Force gain	K_p	2.7634
Reaction force gain	K_{r_1}, K_{r_2}	39.1873,-44.4527
Velocity gain	K_{v_1}, K_{v_2}	144.5613,-60.4529

4.2.1 Force estimation

The DOB using for estimating the disturbance force like the two-mass system. The MEDOB using for estimating the external force on the load side but the block diagram is unlike the two-mass system. As shown in Figure 19.

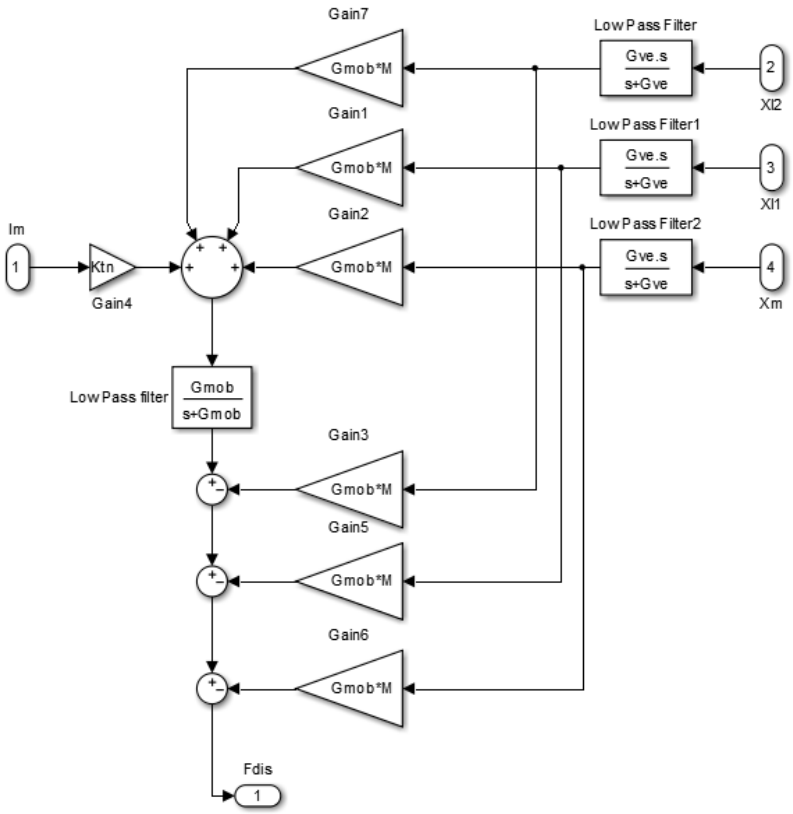

Figure 19 The block diagram of MEDOB for the three-mass system in the simulink.

4.2.2 Force control

The block diagram of the resonance ratio control with MEDOB in the Simulink is shown in Figure 20. In addition, the external force on the load side is the force from the impedance mode (32).

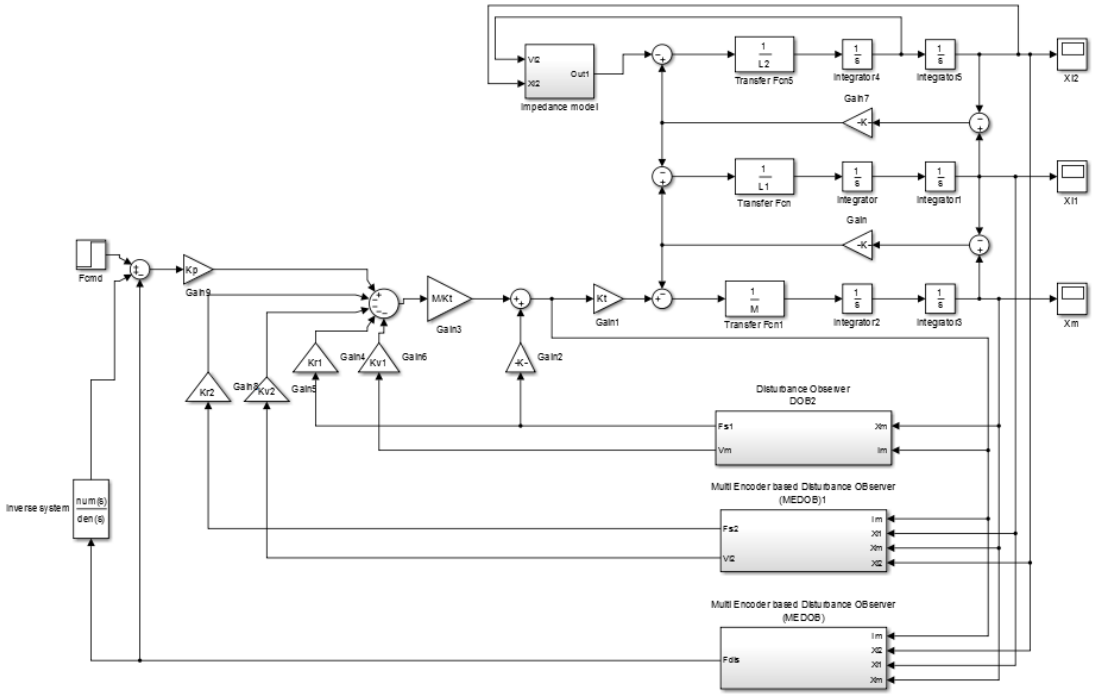

Figure 20 The block diagram of the resonance ratio control with MEDOB of the three-mass system.

The optimum parameters are designed by CDM. They can calculated in MATLAB. Firstly, the parameters must be define the symbolic type. Next, the configuration a_i are equal to the coefficients of characteristic polynomial. Then, the parameters are calculated by CDM with the standard stability indices of Manabe. The source code of design are shown in Figure 21.

```
Define the type of parameters

    syms Kp Kr1 Kr2 Kv1 Kv2 g1 g2 g3 g4 g5 s

Define the parameters

    a0=Ke*Kp*Ks1*Ks2;
    a1=(Ks1*Ks2*Kv1 + Ks1*Ks2*Kv2);
    a2=(Ks1*Ks2 + Kr1*Ks1*Ks2*L1 + Kr1*Ks1*Ks2*L2 + Kr2*Ks1*Ks2*L2);
    a3=(Ks1*Kv1*L2 + Ks2*Kv1*L1 + Ks2*Kv1*L2);
    a4=(Ks1*L2 + Ks2*L1 + Ks2*L2 + Kr1*Ks1*L1*L2);
    a5=Kv1*L1*L2;
    a6=L1*L2;

Calculation

    t=a1/a0;
    g1=(a1^2/(a2*a0));
    g2=(a2^2/(a3*a1));
    g3=(a3^2/(a4*a2));
    g4=(a4^2/(a5*a3));
    g5=(a5^2/(a6*a4));
    [Kp Kr1 Kr2 Kv1 Kv2] = solve(g1 == 2.5, g2 == 2, g3 == 2, g4 == 2, g5== 2, Kp, Kr1, Kr2, Kv1, Kv2)
```

Figure 21 The design code of CDM in the three-mass system.

4.3 Bilateral control

Then, the resonance ratio control is applied to control force in bilateral control. The block diagram of this method is shown in Figure 22.

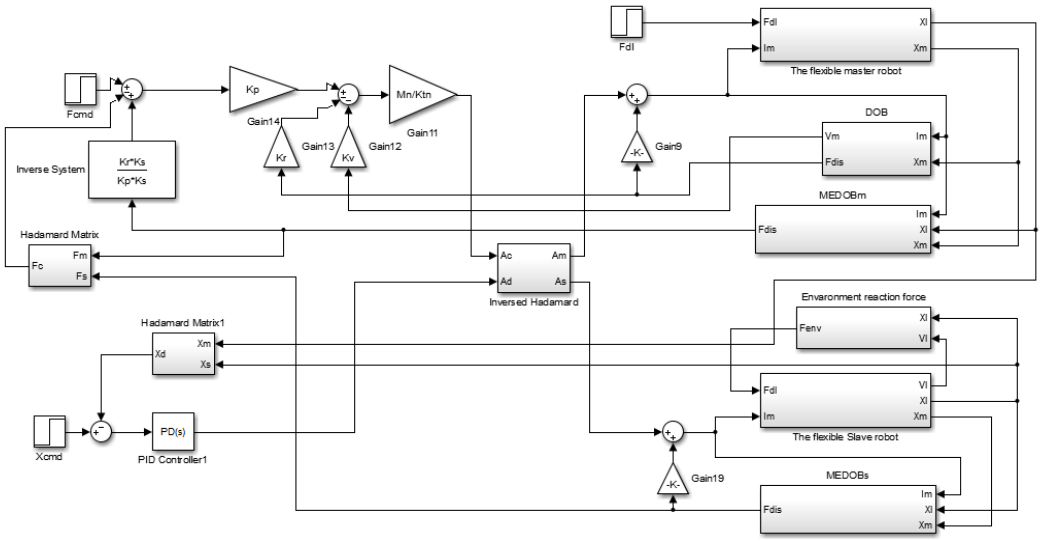

Figure 22 The block diagram of the bilateral control with resonance ratio control.

RESULTS AND DISCUSSION

Results

In this study, the Simulink on MATLAB program is used to simulate the experiments which consisted of the two - mass system and the three - mass system. In each of system, the PID controller, Resonance ratio control and PID controller with resonance ratio control are applied to compare the effectiveness of the proposed method. In addition, the Resonance ratio control applied to the force control of bilateral control in two - mass system.

1. Two – mass system

In this thesis, the results of the simulation in the Simulink on MATLAB program are shown in the Figure 23 and Figure 31.

1.1 Force estimation in the two-mass system with MEDOB

1.1.1 MEDOB without the force control

The noise and vibration is appeared in the force response which is used only MEDOB to estimate the external force. On the other hand, the noise is suppressed in the force response by using MEDOB with the disturbance compensation. The results of MEDOB in the two-mass system without force control are shown in Figure 23, Figure 24 and Figure 25. Where $\boldsymbol{F_{dl}}$ and $\boldsymbol{F_{dis}}$ are the external force and the estimated external force, respectively.

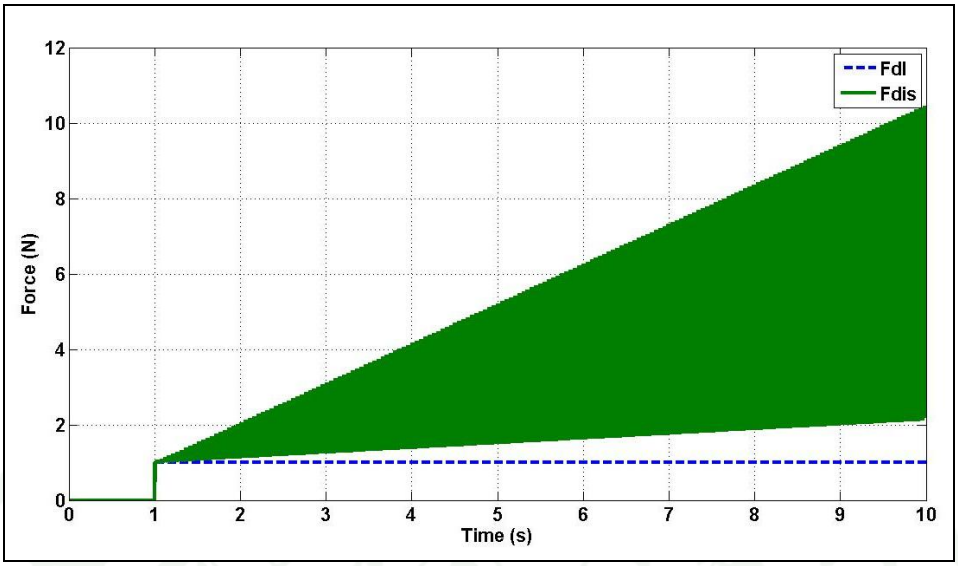

Figure 23 The force response without compensate of MEDOB.

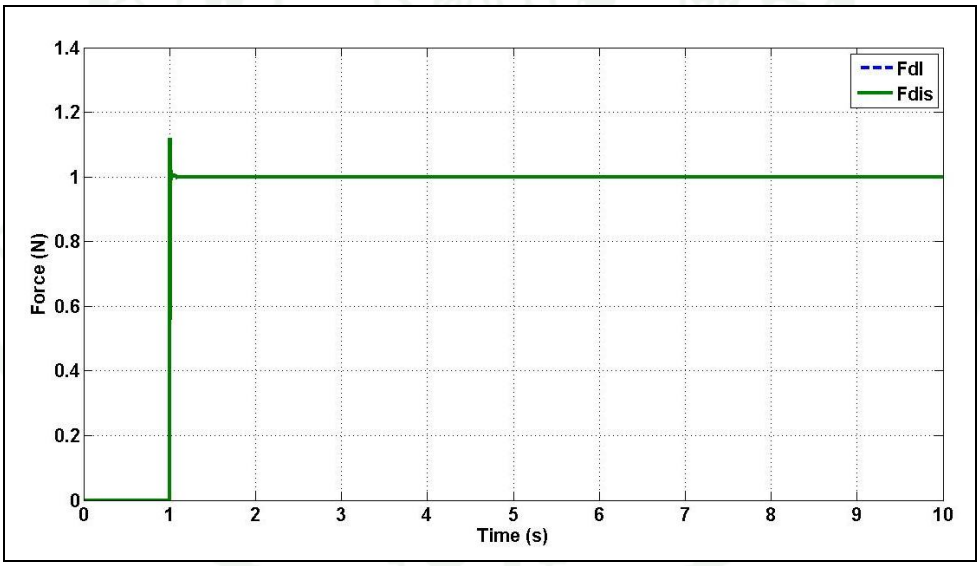

Figure 24 The force response with compensate of MEDOB.

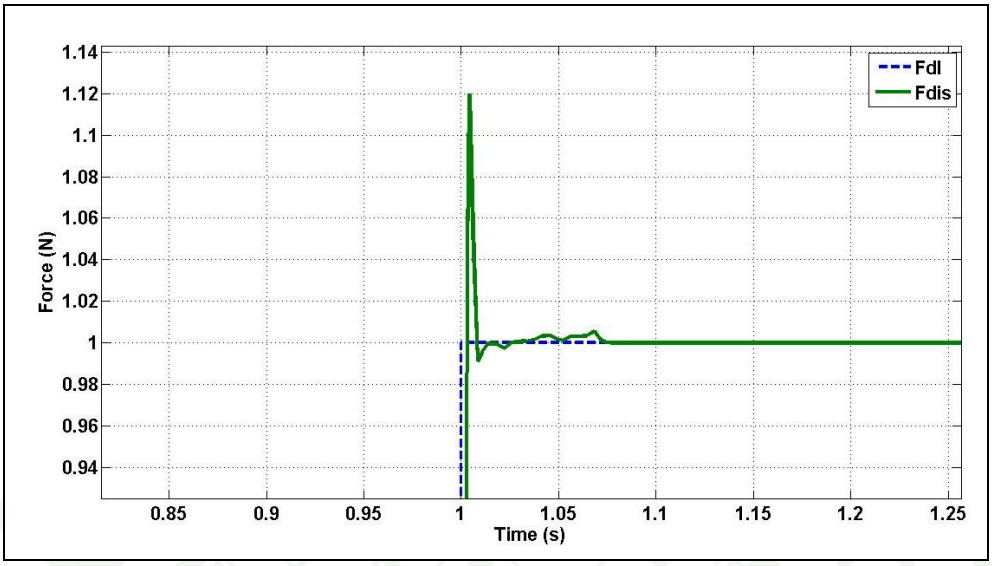

Figure 25 The force response with compensate zoom of Figure 22.

1.1.2 MEDOB with the force control

The force response by using only MEDOB and MEDOB with the force compensation have the noise and vibration as same as the above method. The results of MEDOB in the two-mass system with force control are shown in Figure 26 and Figure 27. Where $\boldsymbol{F}_{cmd}$ and $\boldsymbol{F}_{res}$ are the force command and the force response, respectively. The different environments affect the different force response in force control. The reaction force from the environments is given by the impedance model (32).

The force response from the different environments such as (K_{ss}, K_{dd}) equal to $(1000,100),(500,50),(250,25)$ and $(100,10)$ as shown in Figure 27, Figure 28, Figure 29 and Figure 30, respectively.

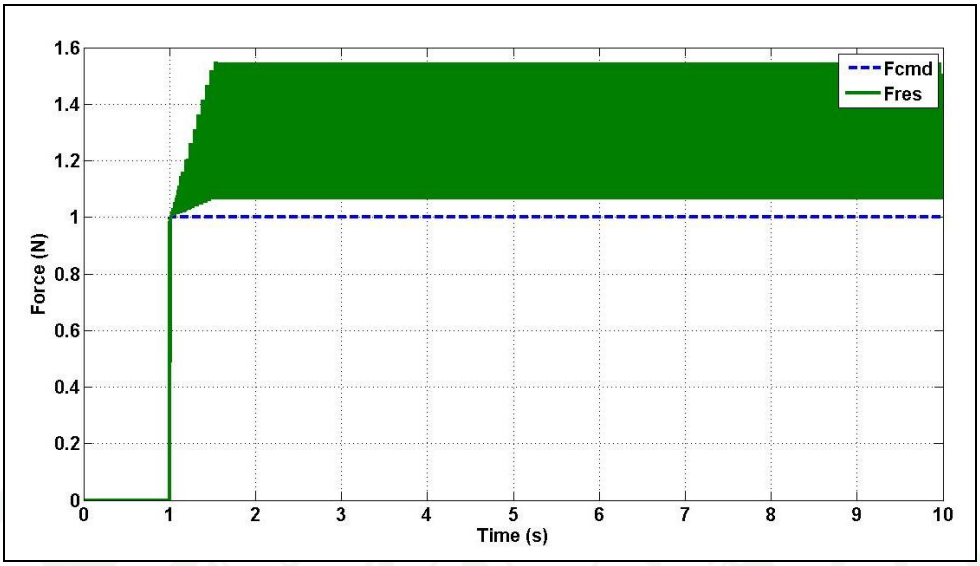

Figure 26 The force response without compensate in the force control.

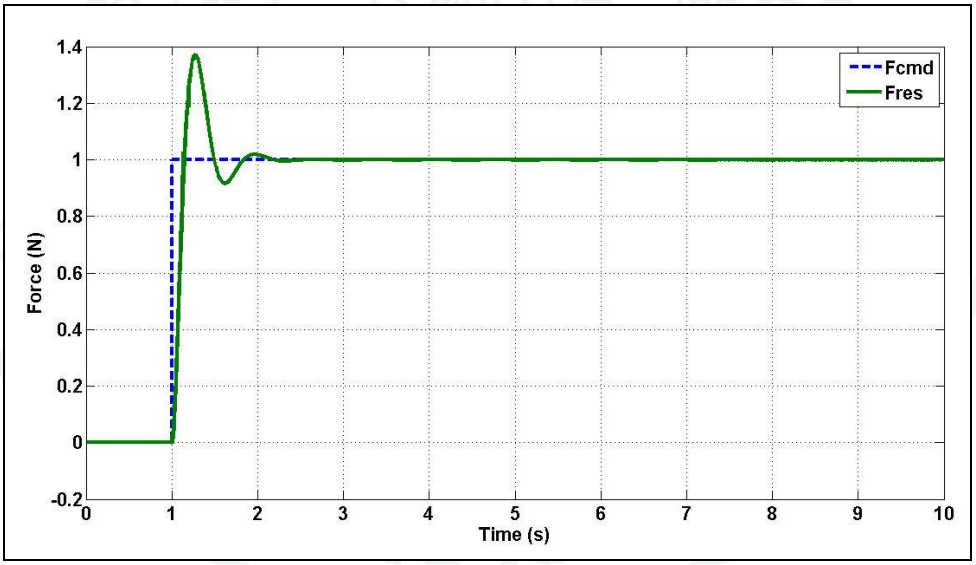

Figure 27 The force response with compensate in the force control (K_{ss} = 1000, K_{dd} = 100).

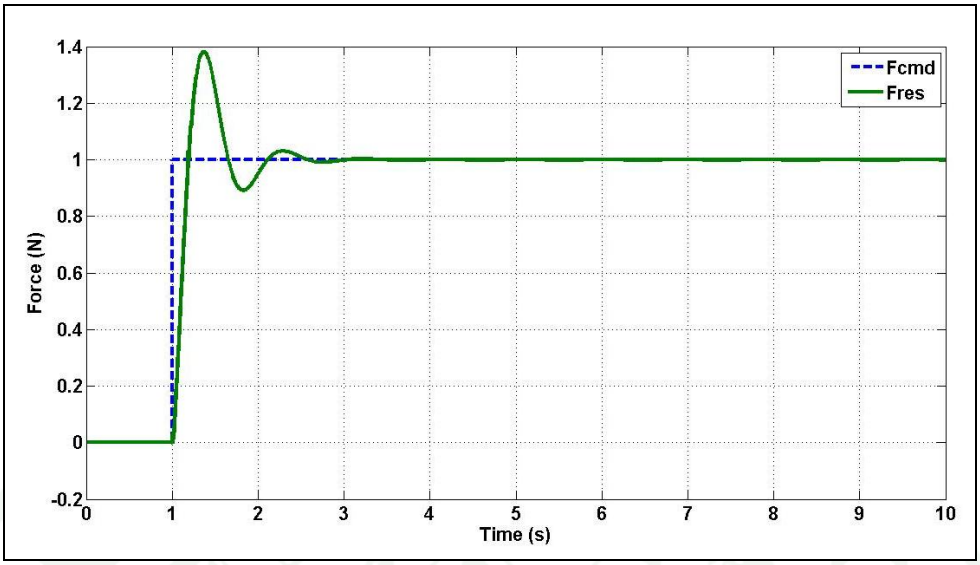

Figure 28 The force response of the environment (K_{ss} = 500, K_{dd} = 50).

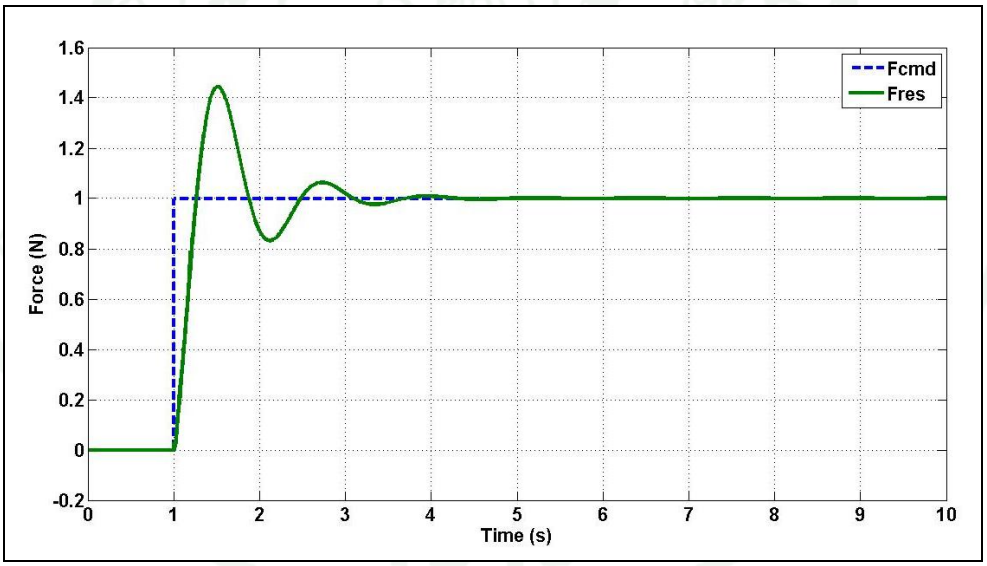

Figure 29 The force response of the environment (K_{ss} = 250, K_{dd} = 25)**.**

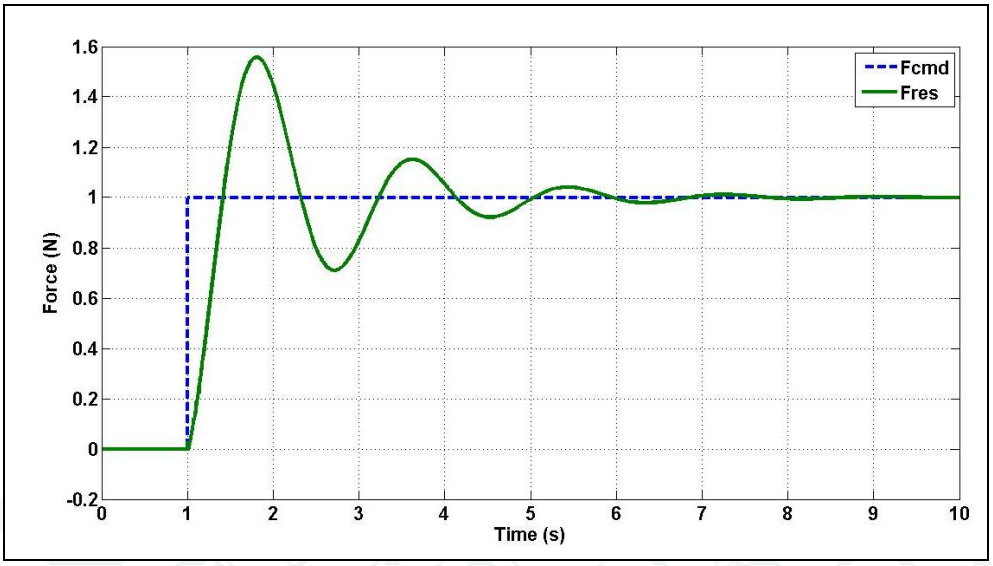

Figure 30 The force response of the environment (K_{ss} = 100, K_{dd} = 10)**.**

From Figure 29 and Figure 30, the force response has more overshoot but less in the setting time in the hard environment. On the other hand, the soft environment has less overshoot but more in the setting time.

1.2 Resonance ratio control

By using the conventional PID controller, the overshoot in the force response is occurred. On the other hand, the force response of the resonance ratio control with CDM does not have overshoot and vibration as shown in Figure 31.

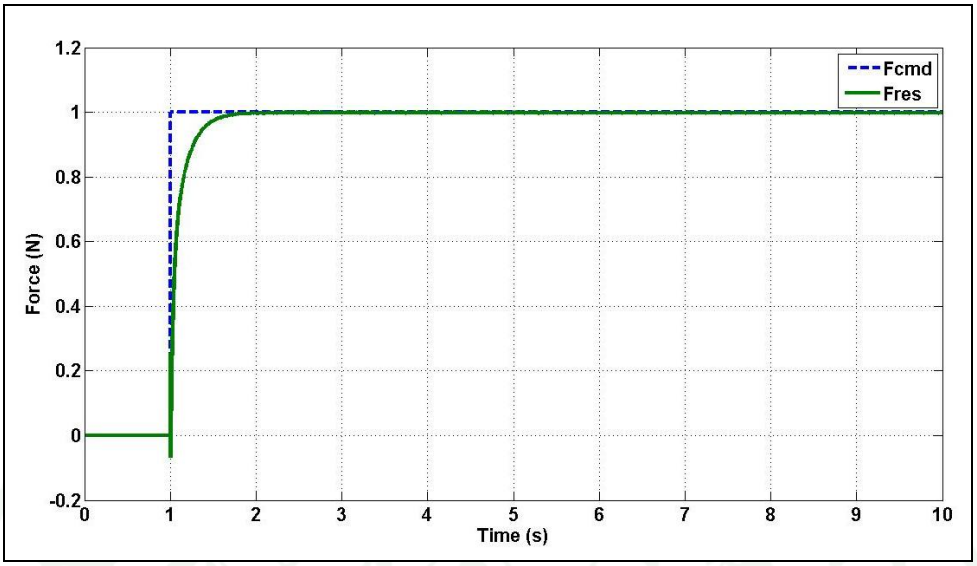

Figure 31 The force responce of resonance ratio control in the two-mass system.

2. Three – mass system

In three-mass system, the external force which estimated by MEDOB is used to feedback in the force control. The force response by using the conventional PID controller is not good enough. For example, there are the vibration and the overshoot. When applying the resonance ratio control in PID controller, the responses are shown in Figure 30 and Figure 31. Where $\boldsymbol{F}_{res(PID)}$ and $\boldsymbol{F}_{res(PID-RRC)}$ are the force response by using the conventional PID controller and the force response by using the PID controller with the resonance ratio control, respectively.

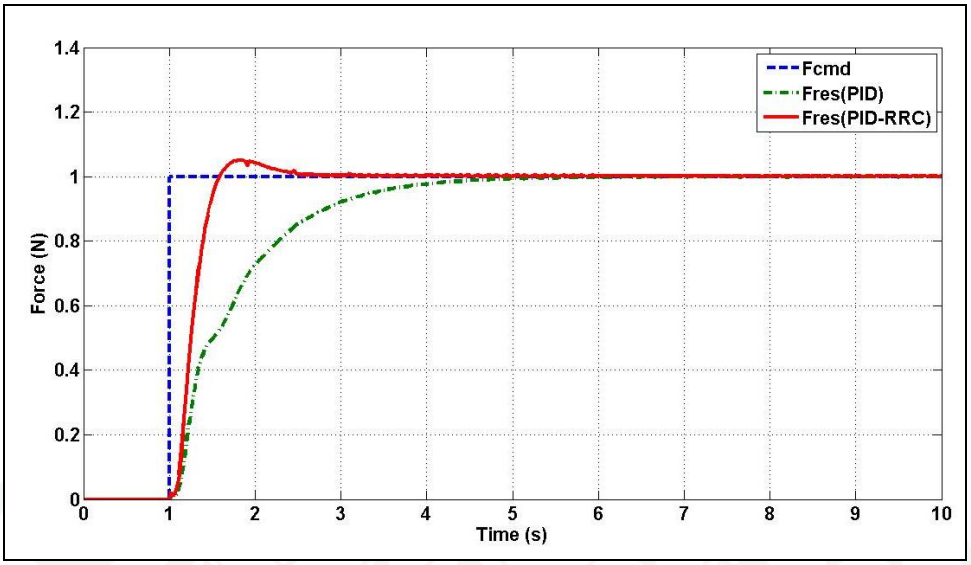

(a) Soft environment.

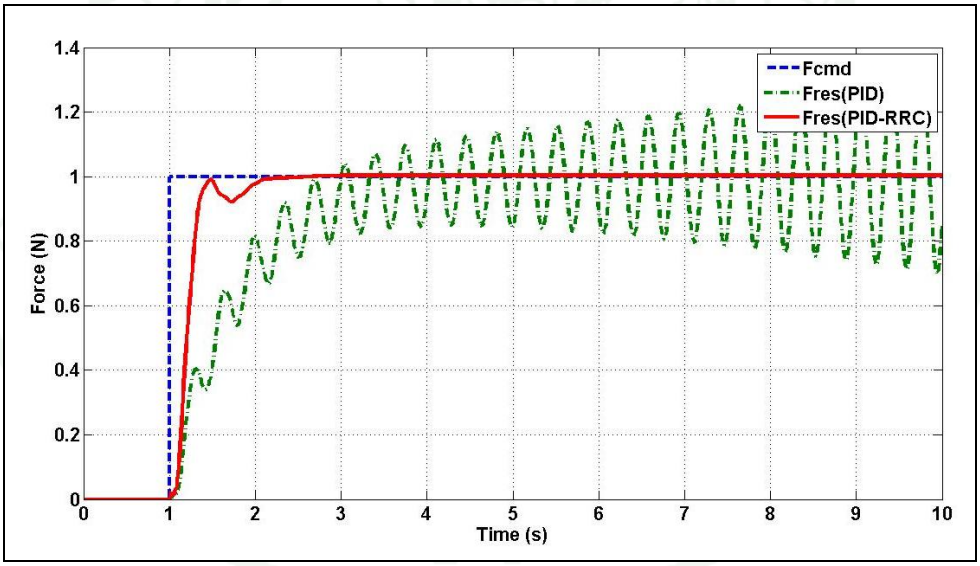

(b) Hard environment.

Figure 32 The force response of the three-mass system in the different environment

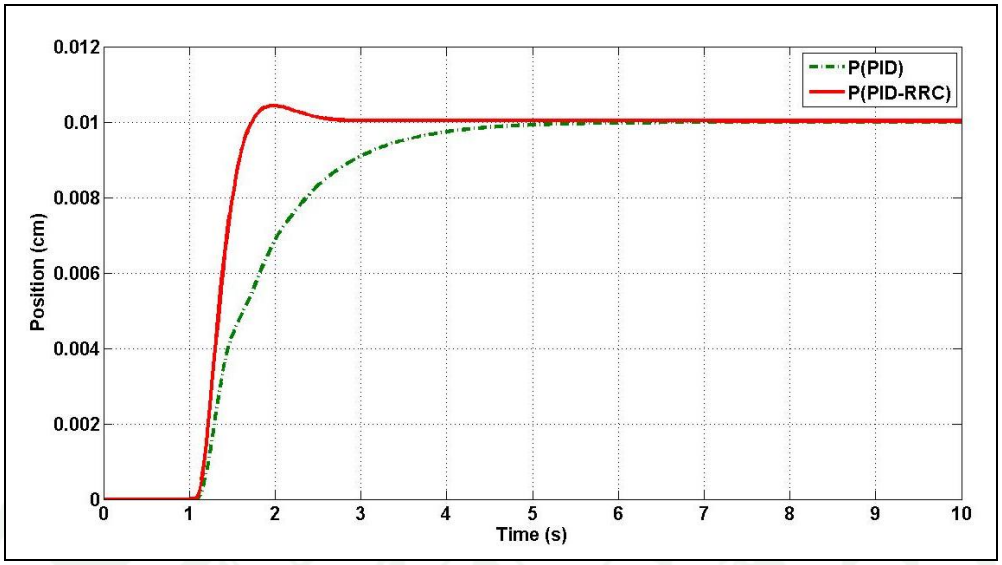

(a) Soft environment.

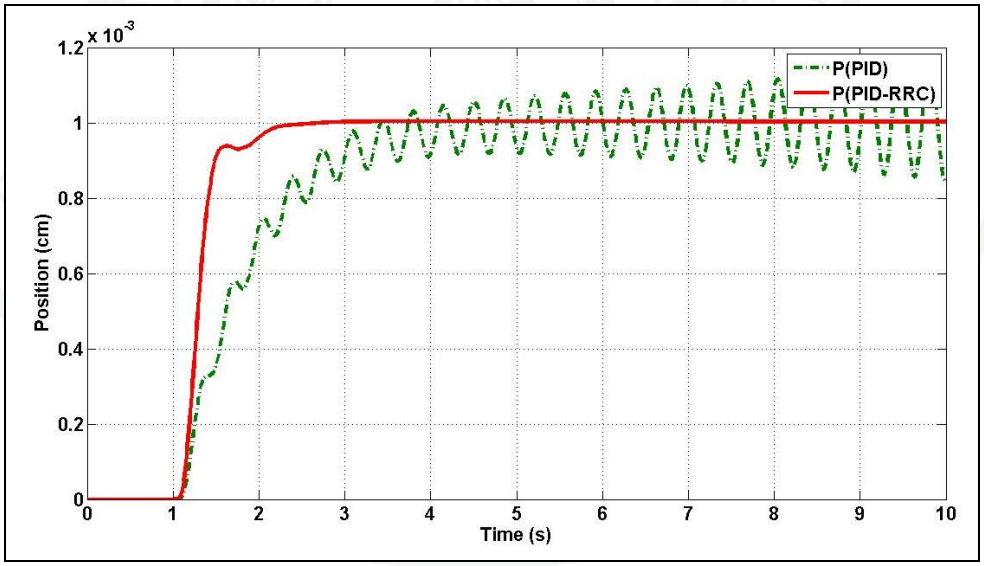

(b) Hard environment.

Figure 33 The position response of the three - mass system in the different environment

In Figure 32 and Figure 33 the vibration of force and position response in the soft environment are smaller than the hard environment. The vibrations are reduced by using PID controller with resonance ratio control in the both environment.

The PID controller with resonance ratio control has an overshoot. So, the resonance ratio control with coefficient diagram method is used to control. This method can be used to guarantee the robustness and good performance in the different environment as shown in Figure 34.

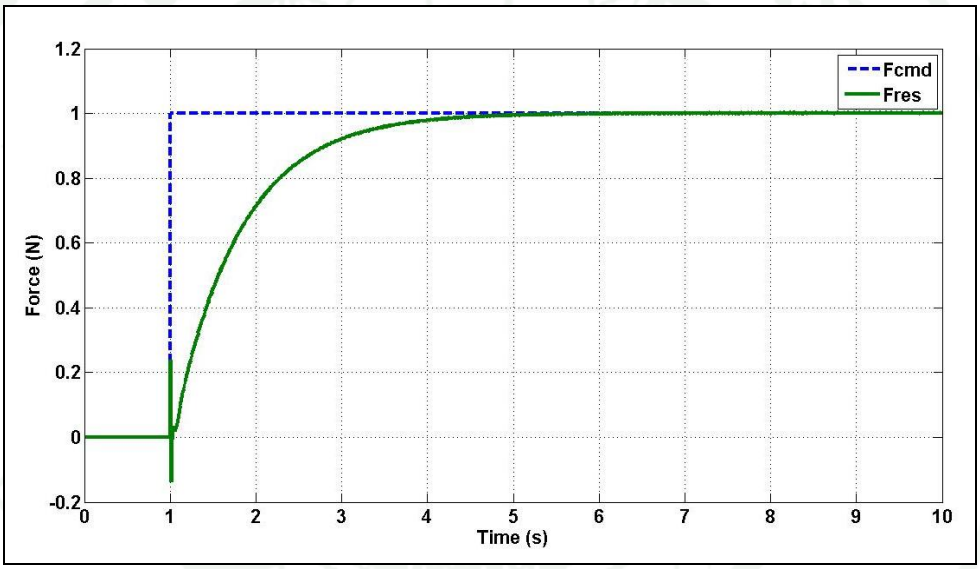

(a) Soft environment.

Figure 34 The force response of the three-mass system with resonance ratio control in the different environment.

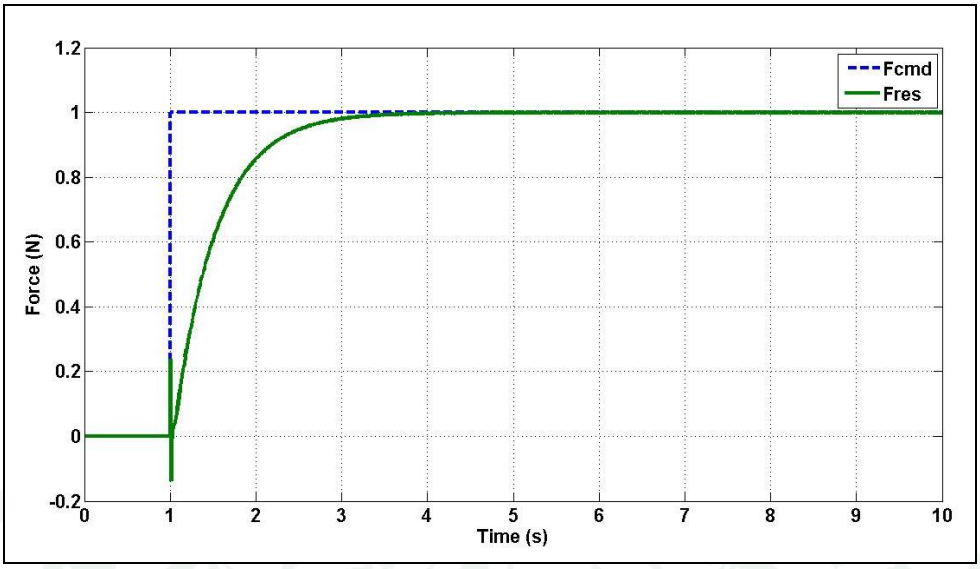

(b) Hard environment.

Figure 34 (Continued)

3. Bilateral Control

The force and position responses of the bilateral control have improved since the resonance ratio control and CDM are used to control the force of the two-mass system as shown in Figure 35 and Figure 36, respectively. Where F_{master} , F_{slave} P_{master} and P_{slave} are the force response and the position response on the master and slave side, respectively.

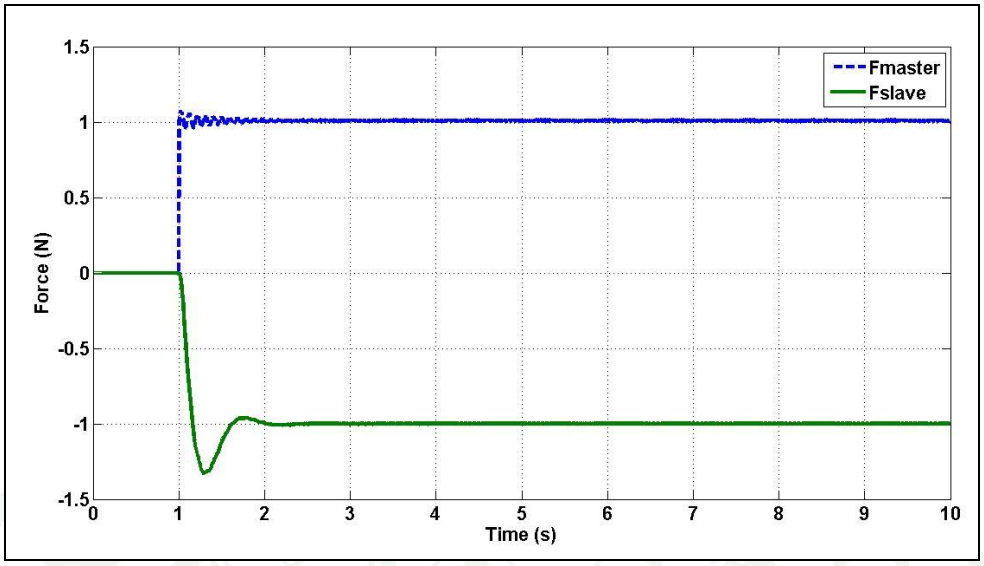

Figure 35 The force response of the PID controller

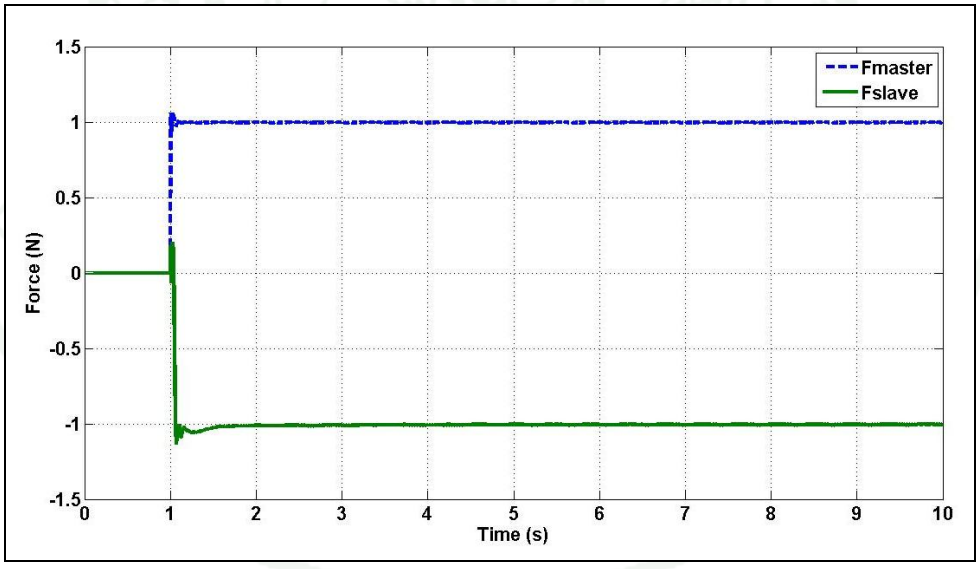

Figure 36 The force response of the bilateral control in the two-mass system

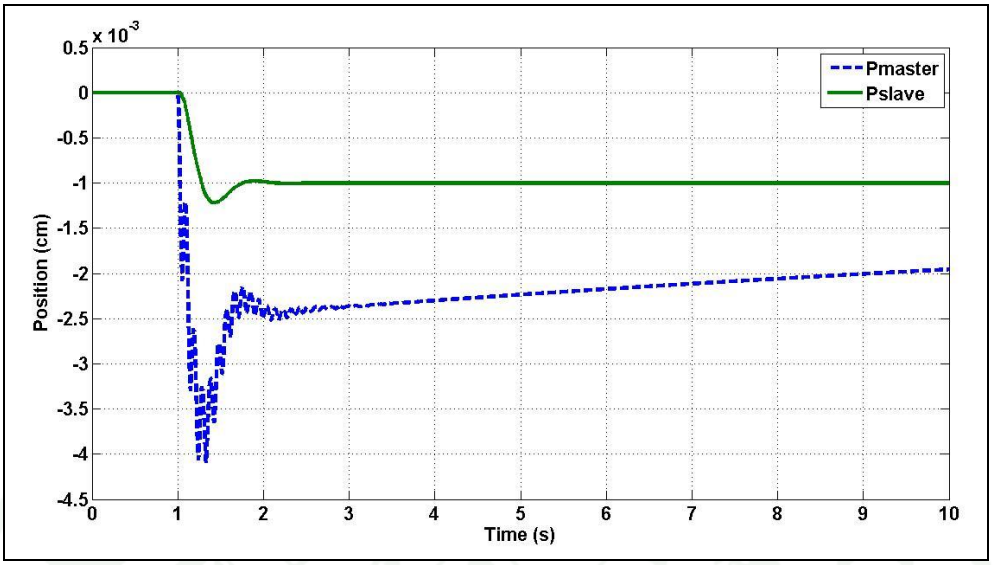

Figure 37 The position response of the PID controller.

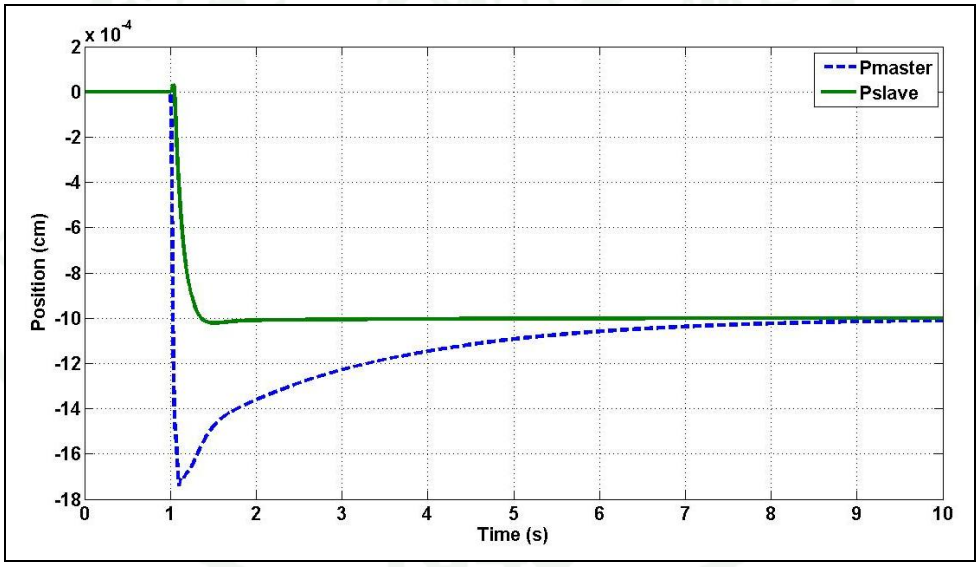

Figure 38 The position response of the bilateral control in the two-mass system.

The force response bilateral control using resonance ratio control with CDM can better control force by reducing the vibration. As seen in Figure 35 and Figure 36, is the force response of the conventional PID control and the force response of master side is opposite of slave, in the way of Newton's law. In addition, this method can control the position much better by reducing an error, as shown in Figure 37 and Figure 38.

Discussions

1. Two - mass system

1.1 Force estimation.

The result of the experiment, the MEDOB can estimate external force if there is the force control but if there is no force control; the MEDOB cannot estimate the external force. However, the MEDOB requires disturbance compensate loop to estimate external force.

1.2 Effect of difference environment.

In the hard environment, the force response has more overshoot but less in the setting time. On the other hand, the soft has less overshoot but more in the setting time.

1.3 Force response.

From the resonance ratio control with CDM will rid of vibration and reduce setting time.

2. Three - mass system

2.1 Force response.

From using the PID controller with the resonance ratio control, the vibration is reduced in both soft and hard environment and the convention PID controller always vibrate in the hard environment.

From using the resonance control with CDM, the vibration will be suppressed in both soft and hard environment. But in soft environment, the setting time is slower than hard environment.

CONCLUSION AND RECOMMENDATIONS

Conclusion

From the experimental results and discussion of this study, the conclusion can be drawn as follow:

1. Although, the DOB and the MEDOB are able to estimate the external force but appropriate cut-off frequency need to be identify to acquire robust performance.

2. The external force on the motor side, which is estimated by DOB, compensated in the acceleration dimension in the motor side. In addition, the external force on the load side can be estimated by MEDOB instead of the force sensors in two and three mass system.

3. The resonance ratio control can suppress the vibration of the flexible structure and hard environment. Because this method has a feeding back the estimated reaction force to the motor in acceleration dimension. In addition, the system is controllable when the frequency has increased. Therefore, this method helps to improve the better performance.

Recommendation

1. This method has an error on the high frequency input because it has a slow transient. If this method can develop the transient, it will have more advantages for the robot in the future.

2. In the future, Kalman-filter will work together with the DOB and the MEDOB for estimating force to get accuracy and precision.

LITERATURE CITED

Abeygunawardhana, P. K. W. and T. Murakami. 2010. Vibration Suppression of Two-Wheel Mobile Manipulator Using Resonance-Ratio-Control-Based Null-Space Control. **IEEE Transactions On Industrial Electronics** 57 (12): 4137-4146.

Back, J. and H. Shim. 2008. Adding Robustness to Nominal Output-Feedback Controllers for Uncertain Nonlinear Systems: A Nonlinear Version of Disturbance Observer. **Automatica** 44 (10): 2528-2537.

Brigante, C. M. N., N. Abbate, A. Basile, A.C. Faulisi and S. Sessa. 2011. Towards Miniaturization of a Mems-Based Wearable Motion Capture System. **IEEE Transactions On Industrial Electronics** 58 (8): 3234-3241.

Ferretti, G., G. A. Magnani and P. Rocco. 2004. Impedance Control for Elastic Joints Industrial Manipulators. **IEEE Transactions On Robotics and Automation**. 20 (3): 488-498.

Garcia, J. G., A. Robertsson, J. G. Ortega and R. Johansson. 2008. Sensor Fusion for Compliant Robot. **IEEE Transactions On Motion Control Robotics** 24 (2): 430-441.

Jaechan, L. and D. Hong. 2010. Cost Reference Particle Filtering Approach to High-Bandwidth Tilt Estimation. **IEEE Transactions On Industrial Electronics** 57 (11): 3830-3839.

Katsura, S., J. Suzuki and K. Ohnishi. 2006. Pushing Operation by Flexible Manipulator Taking Environmental Information into Account. **IEEE Transactions On Industrial Electronics** 53 (5): 1688-1697.

Katsura, S., Y. Matsumoto and K. Ohnishi. 2007. Modeling of Force Sensing and Validation of Disturbance Observer for Force Control. **IEEE Transactions On Industrial Electronics** 54 (1): 530-538.

Katsura, S., K. Irie and K. Ohishi. 2008. Wideband Force Control by Position-Acceleration Integrated Disturbance Observer. **IEEE Transactions On Industrial Electronics** 55 (4): 1699-1706.

Kubo, R. and K. Ohnishi. 2009. Mechanical Recognition of Unknown Environment Using Active/Passive Contact Motion. **IEEE Transactions On Industrial Electronics** 56 (5): 1364-1374.

Linda, O. and M. Manic. 2011. Self-Organizing Fuzzy Haptic Teleoperation of Mobile Robot Using Sparse Sonar Data. **IEEE Transactions On Industrial Electronics** 58 (8): 3187-3195.

Mitsantisuk, C., K. Ohishi and S. Katsura. 2012a. Estimation of Action/Reaction Forces for the Bilateral Control Using Kalman Filter. **IEEE Transactions On Industrial Electronics** 59 (11): 4383-4393.

Mitsantisuk, C., K. Ohishi and S. Katsura. 2012b. Control of Interaction Force of Twin Direct-Drive Motor System Using Variable Wire Rope Tension with Multisensor Integration. **IEEE Transactions On Industrial Electronics** 59 (1): 498-510.

Mitsantisuk, C., M. Nandayapa, K. Ohishi and S. Katsura. 2012c. Resonance Ratio Control Based on Coefficient Diagram Method for Force Control of Flexible Robot System, pp. 1-6. **IEEE 12th International Workshop On Advanced Motion Control (Amc), 2012.**

Natori, K., T. Tsuji, K. Ohnishi, A. Hace and K. Jezernik. 2010. Time-Delay Compensation by Communication Disturbance Observer for Bilateral Teleoperation under Time-Varying Delay. **IEEE Transactions On Industrial Electronics** 57 (3): 1050-1062.

Ohba, Y., M. Sazawa, K. Ohishi, T. Asai, K. Majima, Y. Yoshizawa and K. Kageyama. 2009. Sensorless Force Control for Injection Molding Machine Using Reaction Torque Observer Considering Torsion Phenomenon. **IEEE Transactions On Industrial Electronics** 56 (8): 2955-2960.

Oishi, K., K. Onishi and K. Miyachi. 1984. An Approach to the Torque-Speed Regulation of the Separately Excited Dc Motor Using a State Observer. **Electrical Engineering in Japan** 104 (3): 93-99.

Pereira, E., S.S. Aphale, V. Feliu and S.O.R. Moheimani. 2011. Integral Resonant Control for Vibration Damping and Precise Tip-Positioning of a Single-Link Flexible Manipulator. **IEEE/Asme Transactions On Mechatronics** 16 (2): 232-240.

Puangmali, P., K. Althoefer and L.D. Seneviratne. 2010. Mathematical Modeling of Intensity-Modulated Bent-Tip Optical Fiber Displacement Sensors. **IEEE/Asme Transactions On Instrumentation and Measurement** 59 (2): 283-291.

Salvatore, N., A. Caponio, F. Neri, S. Stasi and G.L. Cascella. 2010. Optimization of Delayed-State Kalman-Filter-Based Algorithm Via Differential Evolution for Sensorless Control of Induction Motors. **IEEE/Asme Transactions On Industrial Electronics** 57 (1): 385-394.

Shunji, M. 1998. The Coefficient Diagram Method. **Ifac Symposium on Automatic Control in Aerospace** 14: 199-210.

Strolz, M., R. Groten, A. Peer and M. Buss. 2011. Development and Evaluation of a Device for the Haptic Rendering of Rotatory Car Doors. **IEEE Transactions On Industrial Electronics** 58 (8): 3133-3140.

Suwanratchatamanee, K., M. Matsumoto and S. Hashimoto. 2011. Haptic Sensing Foot System for Humanoid Robot and Ground Recognition with One-Leg Balance. **IEEE Transactions On Industrial Electronics** 58 (8): 3174-3186.

Tsuji, T., Y. Kaneko and S. Abe. 2009. Whole-Body Force Sensation by Force Sensor with Shell-Shaped End-Effector. **IEEE Transactions On Industrial Electronics** 56 (5): 1375-1382.

Yalcin, B. and K. Ohnishi. 2009. Infinite-Mode Networks for Motion Control. **IEEE Transactions On Industrial Electronics** 56 (8): 2933-2944.

Yokokura, Y., S. Katsura and K. Ohishi. 2009. Stability Analysis and Experimental Validation of a Motion-Copying System. **IEEE Transactions On Industrial Electronics** 56 (10): 3906-3913.

Yuki, K., T. Murakami and K. Ohnishi. 1993. Vibration Control of 2 Mass Resonant System by Resonance Ratio Control. **Industrial Electronics, Control, and Instrumentation, 1993; Proceedings of the Iecon '93., International Conference On** 2009-2014 vol.2003.

CURRICULUM VITAE

NAME : Mr. Phalakorn Kladjaroen

BIRTH DATE : March 23, 1990

BIRTH PLACE : Samutsakhon, Thailand

EDUCATION :

YEAR	INTITUTE	DEGREE/DIPLOMA
2012	Kasetsart Univ.	B.Eng. (Electrical)

POSITION/TITLE : Graduate student

WORKPLACE : Faculty of Engineering, Kasetsart University

SCHOLARSHIP/AWARDS : Teaching assistantship scholarship form The Graduate School Kasetsart University (2013)

PUBLICATIONS :

[1] พลากร กลัดเจริญ, เชาวลิต มิตรสันติสุข และ K. Ohishi. 2556. การลดการสั่นสะเทือนin หุ่นยนต์มาสเตอร์-สเลฟ ที่มีความยืดหยุ่นโดยวิธีการควบคุมอัตราการสั่นพ้อง จากวิธีแผนผังค่าสัมประสิทธิ์, 727-730. ใน **การประชุมวิชาการทางวิศวกรรมไฟฟ้า ครั้งที่ 36** ณ เฟลิกซ์ริเวอร์แคว รีสอร์ท จ.กาญจนบุรี

[2] Kladjaroen, P., C. Mitsantisuk, S. Jarudamrongsak and K. Hongesombut. 2014. Vibration Suppression of Flexible Three-Mass System Using PID Controller Based on Resonance Ratio Control, pp. 550-553. *In* **The 29th International Technical Conference on Circuits/Systems, Computers and Communications.** 1-4 July 2014, Phuket Graceland Resort and Spa Phuket, Thailand.